DESIGN AND IMPLEMENTATION OF FULL SOLID STATE HIGH VOLTAGE NANOSECOND PULSE GENERATORS

by

Tao Tang

A Dissertation Presented to the
FACULTY OF THE GRADUATE SCHOOL
UNIVERSITY OF SOUTHERN CALIFORNIA
In Partial Fulfillment of the
Requirements for the Degree
DOCTOR OF PHILOSOPHY
(ELECTRICAL ENGINEERING ELECTRO-PHYSICS)

May 2008

Dedication

To my parents

Acknowledgments

First of all, I would like to express my deep gratitude toward Prof. Martin A. Gundersen, my PhD adviser, for all the advices, all the supports and all the encouragements that he has given me.

I would like to thank all the help from Dr. Kuthi and all other colleagues at Pulsed Power Lab at University of Southern California.

I would like to thank Professors John Choma, Thomas C. Katsouleas, Stephan Haas, and Hossein Hashemi for serving on my Ph.D advisory committee and Professors Eun Sok Kim, and Stephan Haas for serving on my Ph.D defense committee.

I would like to thank our collaborators:

Dr. Edward B. Garon and Professor H. Phillip Koeffler at David Geffen School of Medicine at UCLA.

Dr. Tomonori Urushihara, and Dr. Taisuke Shiraishi, at Nissan Research Lab.

Last but not least I would like to thank my dear friends and families. This work would not have been possible without your love, understanding and support.

This work was primarily funded by the Compact-Pulsed Power MURI program funded by the Director of Defense Research and Engineering (DDR&E) and managed by the Air Force Office of Scientific Research (AFOSR) and was also

funded by the Army Research Office (ARO) and Office of Naval Research (ONR) and also partly funded by Nissan Research Lab.

Table of Contents

List of Figures

List of Tables

Abstract

As a scheme of delivering accumulated energy in short period of time to gain high instant power, pulsed power technology is widely used to generate high power transient electric pulses. In recent years, low energy (tens of mJ to a few J per pulse) nanosecond range pulse width applications such as electroperturbation of cells, food disinfection, and pollution reduction gain a lot of attention. The improvement of solid state switches makes it possible to build a full solid state pulsed power unit to generate nanosecond pulses. Comparing with traditional gas switch generators, the solid state generators have the merits of high reliability, long life time, simple supporting circuitry and less cost.

In this dissertation, solid state pulsed power systems will be discussed in system, device and topology levels and several application-specific nanosecond high voltage pulse generators are presented.

First, pulsed power system is investigated on a system level. Three major sub-systems and their abstract models are introduced. Then, typical solid state electrical components for pulsed power system are discussed. After that, several typical pulse-forming topologies are introduced as fundamental building blocks for pulsed power system.

Special designed Diode Opening Switch (DOS) is able to generate nanosecond megavoltage range pulses. A modified topology is invented to use commercial off-the-shelf (COTS) diode and get comparable performance. This method makes it possible to make a compact pulsed power system generating nanosecond pulses with several kVs amplitude.

Based on this new topology, three pulse generators are designed: One pulser is designed for electroperturbation study, which is able to deliver 7.5 kV 5ns pulses into 10 ohm load. The second one is designed for localized skin cancer therapy research which takes 50 ohm catheter load and generates 6kV 20ns pulses. The third one is developed for transient plasma ignition which used in a single cylinder test engine and delivers 60kV 20ns pulses.

Inspired by studies in pulsed electric field gas discharge imaging, a new topology of pulse adding is invented for transient plasma ignition. A pulse adding system is built on this topology and demonstrated in a pulsed detonation engine testing system.

Chapter 1 Introduction

Pulsed power is a scheme where energy stored over a long period of time is delivered into a load in a much shorter time scale.

The definition implies a fundamental characteristic of pulse power system: high peak-to-average power ratio or high instantaneous power. This unique characteristic makes pulsed-power techniques successful in applications which are not possible with other methods (pulse power enabling applications) or which will performs better if been pulsed (pulse power improving applications).

The first type of loads can be further divide into three categories: 1. Competing heating/charging effect need to be suppressed to enable the study of material properties under high electric/magnetic field; 2. When duration of transient high power is shorter than relaxation time, the load can be pumped into a state far from equilibrium; 3. Short high power peak can be seen as “delta function” and used to take a snapshot of fast process. For the second type, mostly are the process naturally “pulsed”, like electromagnetic launcher system. Table 1.1 shows some typical applications.

Table 1.1 *Typical applications of pulsed power systems*

Function	Suppress competing effect	Introduce non-equilibrium state	Sampling fast process	Increase performance
Application	Electroporalation of cell, Manipulate seeds, Disinfection	Streamer discharge, Pumping laser	Pulsed X-ray imaging	EM Launcher, Flash light

1.1 History of pulsed power

The first modern pulsed power system was developed by John Chiristopher (Charlie) Martin and this colleagues at the Atomic Weapon Establishment in 1960s. Such system is proved to be very useful and efficient in the circumstances where transient high power is needed. After its invention, pulsed power science and technology rapidly disseminated to the United States, former Soviet Union and the present-day Russia, Europe, and Asia. At the early age, pulsed power was mainly used in the gigantic system like accelerator, fusion research, laser system and electro-magnetic weapon research. Nowadays, powered power is widely spread into civil low energy compact systems like the ignition system in automobile and biological researches.

Since World War II, the development of pulsed power has mainly been driven by military requirements, both for the advancement of pulsed-power-based weapons and for the evolution of new simulation and diagnostic tools. Considerable effort has been undertaken to develop pulsed-power-based weapon systems such as

electromagnetic mass launchers and beam weapons. Despite this effort, except for pulsed radar, no weaponised pulsed-power system has yet evolved. But many systems have been built for military research and development programmers to study the effects of nuclear weapons, to determine the properties of materials under extreme shock wave loading, and to create strong pulses of hard X-rays to image fast explosives.

Recent progress in the development of reliable and affordable components for pulsed-power systems such as long-lived high-voltage capacitors and new types of high-power semiconductor switches has created new interest in utilizing pulsed-power techniques for commercial and industrial purposes. In contract to some military applications, economic considerations have the strongest impact on commercialization.

1.2 Biological and medical application

Recently, both biological cell modeling and experimental observations have indicated that exposure of mammalian cells to ultra-short (several to tens nanosecond), high strength (several mega volts per meter) pulsed electric fields can trigger programmed cell death (apoptosis,) through intracellular effects that are distinct from classical electroporative effect. Such a natural destructive process,

referred to here as nano-electroperturbation, is of interest for potentially cancer therapy.

High voltage nanosecond electric pulse is essential to the electroperturbation study of biological cells. The response of the cells upon electric pulse exposure depends on the pulse width and amplitude. Pulse longer than 1μs normally results in electroporation, which stands for opening of pores on outer cell membrane temporarily or permanently. When the duration of the pulse reduced to nanosecond range, the cell nuclei can be affected without adversely affecting the outer cell membrane. Further experimental investigations of electroperturbation require compact pulse generators with readily variable output parameters.

At this moment, most pulsed power systems for nano-electroperturbation research are developed in two research laboratories at University of Southern California and Old Dominion University. According to the electrical load applied to, they fall into three categories: 1) pulse generators are used to observe the immediate effect of ultra short pulse in live cells under a fluorescence microscope; 2) pulse generators are developed to treat million cells in standard electroporation cuvette to collect statistical cell responses; 3) pulse generators are used to deliver electric pulses locally to tissue on a living animal.

The desired pulse amplitude and duration is determined by required electric field and electrode geometry. For example, in order to generate 5-10 MV/m (a

hypothetical threshold field strength for intracellular effects, the value is highly dependent on cell types.) electric field in a standard cuvette load with 1mm electrode gap, pulses with 5-10 kV in amplitude are required. A repetition rate of around 10 Hz is also preferred for the observation of the effects with good statistics.

1.3 Aerospace and automobile application

Plasma-assisted combustion flame ignition and combustion control has interesting properties. It is well-known that applying an electric field to a flame can affect its propagation speed, stability and combustion chemistry. Pulsed corona discharges can create non-thermal plasmas (NTPs) that usually consist of many streamers, efficiently filling the gas volume. The electric field in a streamer wave front can be as high as a few EVs, which is able to generate energetic electrons capable to activate fuel or fuel-oxidizer (e.g., air) mixtures that feed internal combustion engineers, furnaces and other combustion devices. Energetic electrons with high kinetic energies can effectively generate reactive species which can then rapidly initiate or accelerate chain reactions. As an example, nanosecond pulsed corona discharge has been successfully employed for nitrogen oxides removal and aircraft pulsed detonation engines (PDE) ignition by providing sufficient energetic electrons that cause radical enhancement.

Desired pulse amplitude depends on the exact geometry of the combustor, ignition chamber as well as corona electrode. In our case at least 50 kV is needed for effective energy deposition. The pulse length must be longer than the streamer formation time but shorter than the arc formation time. In the present experiments the pulse length is between 20 and 200 ns.

Chapter 2 Overview of pulsed power system

The definition of pulse power in previous chapter suggests that a pulsed power system consists of three main building blocks: a storage unit, a switching unit and a load.

The storage unit will accumulate energy over a certain amount of time and store in various forms like electric energy, magnetic energy, kinetic energy or chemical energy. For a storage unit, there are two fundamental characteristics: maximum energy density and maximum energy release speed. The first characteristic will determine the size of this subunit: the higher the energy density is the smaller the subunit will be. And the second characteristic will determine the maximum peak-average power ratio which is directly related to rise/fall time of the pulse.

After energy being stored, the switching unit will initiate energy releasing, which will also act as a “pulse forming” unit. A switching unit normally has two states with large difference in impedance: a low impedance state (“on” state) and a high impedance state (“off” state). The switch in on state will have low voltage difference across its two ends and current can flow through the switch. While the switch is in off state, it will have large voltage difference across its two terminals and

current flow is forbidden. The key characteristics of a switching element are hold-off voltage and switching speed. The hold-off voltage is the maximum voltage cross the switch before spontaneous conducting, which is directly related to the maximum charging voltage and/or output voltage. The switching speed is the time interval between the state changing which will determine the rise/fall time of the pulses. Connected with other components, a switch will start the formation of pulses.

The shaped pulses need to be delivered to the load through next major unit: load and matching subunit. A load under pulsed power condition can be quite different comparing with that under normal condition. The high electric field causes non-linear effect of the load and makes the impedance of the load vary during a pulse. And the high frequency components introduced by the short pulse width will make parasitic capacitive/inductive components an important role in the load. To maximize the energy or electrical field delivered to the load, an impedance matching scheme is needed. It can be a transmission line to absorb reflected pulses, a transformer to change the effective impedance of the load, or an adding system to increase output voltage.

2.1 Storage subsystem

An ideal storage system for pulsed power application should be able to charge slowly without any energy loss and discharge rapidly to generate high instant power.

The energy storage device suitable for pulsed-power applications should meet the following basic requirements:

Low leakage rate to ensure long storage time and relatively long charging time

High breakdown strength to hold associated high output voltage

High discharge current capability to generate high power

Additional features will be helpful in terms of overall performance, which includes:

Repetition rate capability and long lifetime

High energy density to make system compact

Low specific cost

Some of these requirements may be in conflict and normally a trade-off is necessary based on the application and the spatial/environmental constraints.

In the early days, mechanical storage system like turning wheels is adopted in the pulsed power system for its high energy density and breakdown strength. But the slow energy delivery speed greatly limits the peak-to-average power ratio, which makes it necessary to have intermediate stages to boost peak power. These intermediate stages nullify the minimization effort from its high energy density and make it hard to build a compact system. For this reason, in modern pulsed power system, the mechanical energy storage is seldom used and is replaced by electromagnetic energy storage elements like inductors and capacitors.

There are two major methods to store electromagnetic energy: energy stored in electric field (capacitive storage) and in magnetic field (inductive storage).

2.1.1 Capacitive storage

Electromagnetic energy can be stored in an electric field which is called capacitive storage. The storage medium is normally a capacitor formed by two electrodes separated by dielectric material. The maximum energy density for a capacitor is limited by the properties of that dielectric material. It can be calculated by $w_e = f_{packing} \varepsilon \varepsilon_0 E_{DB}^2 / 2$. Where w_e is the energy density, $f_{packing}$ is packing factor, ε and ε_0 are relative permittivity and permittivity of vacuum, E_{DB} is breakdown strength. In an ideal situation the packing factor is 1, but for real capacitor, the packing density will be lower and we will use $f_{packing}=0.5$ in the following calculation.

Table 2.1 *Properties of some dielectric materials used for insulation of high-voltage capacitors.*

Material	ε_r	E_{DB} **(MV/m)**	$tg(\delta)$	w_e **(kJ/m^3)**
Impregnated paper	3-4	20-80	0.01-0.03	2.7-56.6
Epoxy	3.5	32	0.014	7.9
Mylar	3	40	0.001	10.6
Polypropylene	2.44	25.6	0.0005	3.5
Teflon	2.1	21.6	0.0002	2.2
Kapton	3.4	280(25μm)	0.001	589.7
Plexiglas	3.3	20	0.009	2.9
Transformer oil	3.4	40	0.0002	12
Aluminiumoxide	8.8	12.6	0.01	3.1
Bariumtitanate	1143	3	0.01	22.8
Glass (borosilicate)	4.84	15.7	0.0036	2.6

In Table 2.1, the material properties and maximum energy density of some common dielectric materials are listed. We can see the energy density ranging from several kJ/m^3 to a few hundred kJ/m^3. And this is the physical limit of the dielectric material.

Besides the dielectric breakdown strength, there are also some important or even dominant factors which determine the high-voltage strength of a capacitor. These factors include the making of terminals (shape, area, metal and bonding method), the environment (temperature, pressure humidity) and operation condition (working frequency, charging speed, voltage reversal).

Another important term is the dielectric constant ε. Although it is called "constant", ε is actually changing with frequency. This phenomenon comes from the finite polarization relaxation time of the material. The finite relaxation time introduced a phase shift between the electric field E and electric flux density D. According to Maxwell's Equations, when E and D are in phase, the electric energy is stored in the E-field; while they are out of phase by 90 degree, energy is totally consumed; anything other then these two, part of the energy is consumed. The consumed energy is:

$$w = \frac{\omega}{2} E_0 D_0 \sin\delta \approx \left(\frac{\omega}{2}\right) E_0 D_0 \operatorname{tg}\delta. \quad (2.1)$$

Where ω is working frequency, E_0 and D_0 are amplitude of electric field and electric flux density at frequency ω, δ is the delayed phase angle. Since δ is very small for normal insulating materials, tgδ is used instead of δ to characterize loss and thus it is called loss factor or loss tangent.

2.1.2 Inductive storage

Electromagnetic energy can be stored in the magnetic field which is called inductive storage. The magnetic field is generated by current flow through a conductor. In order to confine the magnetic field, the conductor is normally wound in to helix structure which is called coil or inductor. Stored energy can be calculated by $w_b = B_{\max}^{\ 2} / 2\mu\mu_0$. Here B_{max} is maximum magnetic flux density, μ is relative permeability of the enclosed area, μ_0 is permeability of vacuum. Unlike capacitive storage where E_{max} and ε vary independently and both play an important role in maximum energy density calculation, the determinant factor for inductive energy storage is only B_{max}. Although the difference of μ can be very large for different materials when B is small, μ will drop to about 1 when B is large. This makes μ unimportant in maximum energy density calculation. Magnetic field is generated by current flow: higher the current is, larger B will be. In order to have current flow in a close loop, certain conducting mechanical structure needs to be maintained. However, the conductor is normally not ideal, and will have resistance. Current flowing

through resistor causes energy loss and will heat up the conductor. When the temperature gets higher than melting point of the conductor, the loop can not be maintained. On the other hand, conductor carrying current will experience force in a magnetic field. This force can be so high that the conductor may break and no longer conducting. These two factors will be considered when estimating B_{max}.

One major effect of current flow is Joule heating effect. A normal conductor will have finite conductivity which makes ohmic loss unavoidable. And another source of heat loss is Joule heating at the conductor surface results from eddy currents generated during the diffusion of the magnetic field into the conductor. For a conducting half-space, the surface temperature can be expressed in the general form.

$$c_v \rho T(0,t) = \frac{1}{2\mu_0} B^2(0,t)\vartheta(t), \quad (2.2)$$

Where c_v is the heat capacity per unit mass, ρ is the mass density, $T(0,t)$ is the surface temperature, $B(0,t)$ is the boundary field, and $\vartheta(t)$ is a factor of order unity depending on the form of the pulse. Using data of Cu, we find a value between 50 and 100 T for the maximum B-field, depending on the pulse shape.

To estimate the limitations resulting from mechanical forces, we evaluate the criterion for static containment, which is valid if the charging time (and therefore the duration of the pressure pulse) is larger than the period of oscillation of the containment:

$$\frac{B^2}{2\mu_0} < \Sigma_y \frac{r_o^2 - r_i^2}{r_o^2 + r_i^2}, \quad (2.3)$$

where Σ_y is the yield strength of the containment material, r_o is the outer radius of the cylindrical containment, and r_i is the inner radius. For the case of the thick ($r_o=2r_i$) copper-beryllium (Σ_y=1000N/mm^2) cylinder, we calculate B<38T. In this case the average energy density in the containment, i.e., within the radius r_o amounts to $w_B = 39000 kJ/m^3$. We see that, even if support structures, insulation, etc. are taken into account, the energy density stored in a magnetic field can be about two orders of magnitude higher than that storable in an electric field.

2.1.3 Summary

Although inductive storage has an advantage in energy density comparing with capacitive storage, most modern pulsed power system is still based on capacitive storage. The major reasons are:

A more complex auxiliary unit is necessary in order to achieve high density in inductive storage. A cooling system is needed to dissipate the Joule heat generated by large current. A mechanical supporting unit is necessary to hold the coil against magnetic force. Leakage magnetic field may affect surrounding electronic devices, so a shielding system will be important in such situation.

The resistive loss is much severe in inductive storage system comparing with capacitive one, which greatly reduces the energy hold time. As frequency increases, the skin effect makes it even harder to reduce resistance in inductor.

And for inductive storage system, an opening switch is needed to commute energy to load (which will be discussed in Chapter 2.2); for capacitive storage system, a closing switch is needed. But reliable, repetitive, fast closing switches are easier to build than the opening switches.

Inductive storage is still used in the pulsed power system, not as a main storage unit but as an intermediate storage unit. A good example will be the ignition coil for the spark plug in an automobile.

2.2 Switching and pulse forming subsystem

A switching unit is a two state circuit element with following properties:

1. It has two distinct impedance states: the high impedance state is called “off” state and low impedance state is called “on” state.

2. It can change from one state to the other. The state changing process is called “switching”. There are two directions of state change: from on to off or from off to on, which is called “opening” and “closing” respectively. A circuit element used to make opening/closing switching is called opening/closing switch.

According to Ohm's law, in off state, current through the switch is nearly 0 but voltage across it can be very large; while in on state, voltage is close to 0 and current can be large.

These two state changes can initiate the delivery of stored energy. If the energy delivered delivery time is much shorter comparing with accumulating time, an energy pulse is formed.

Some switches can be controlled to open but not to close. And they are called "open only switches" or simply "opening switches". Similarly, "closing only switch" or "closing switch" can be defined. The switches which can be controlled to switch in both directions are called "bi-directional switches" or "full controllable switches".

2.2.1 Opening switch

Let's consider an inductive storage system. Energy is stored in the magnetic field generated by current flowing through an inductor. In order to deliver the stored energy, current needs to be forced into the load instead of returning to the other end of the inductor. To do so, a circuit element needs to be placed in series with the storage inductor and in parallel with the load. When inductor is charging, majority of current flows through this element instead of the load. Once this path is blocked, since current through an inductor can not change instantly, the full current has to

flow through the remaining branch i.e. the load. Comparing with the definition of opening switch, we know this circuit element is an opening switch.

Charged inductor can be seen as a current source. So power multiplication is achieved by voltage amplification. That is: voltage across the load increases dramatically and overall power $P=V\times I$ then increases accordingly.

Energy loss in this process consists of 2 parts: 1. resistive loss during charging phase; 2. switching loss. During charging phase, loss is characterized by $I^2\times R$. When the device is switching off, voltage will build up on the load gradually. During this time interval, the switch experiences both high current and voltage which will cause switching loss. Faster the switching speed is, smaller the loss will be. Once the switch is fully open, voltage on the switch reaches its maxim value but current drops to nearly 0. Loss in this phase is determined by current sharing between the load and the switch in off state. To minimize loss in the switch, an ideal opening switch should have: 1. low on state impedance; 2. fast switching speed; 3. high off state impedance. It is hard to achieve all these three at same time since some of them are often contradictory to the other. A compromise is normally needed to minimize loss for a specific application.

An opening switch can also be used to stop discharge process when connected in series with the load. In this case it works like a voltage sharing component, which has little voltage drop in on state and large drop in off state. When used like this, any

parasitic inductors in the circuit will dissipate their stored energy in the switch. This energy can generate a very large voltage across the switch and potentially damage the device. A snubber circuit is needed in this case to absorb this energy and protect the switch.

2.2.2 Closing switch

Similarly, to deliver energy stored in a capacitive element, a closing switch is needed. During charging phase, voltage on capacitor builds up and the closing switch will be in off state to isolate the load from charging source. This way voltage on load can remain low when capacitor is charging. The final voltage is also limited by the hold off voltage of the closing switch. After fully charged, the switch will then be closed to initiate energy delivery. Once the switch changes to on state, the charged capacitor will work as a voltage source connected to the load through the switch. When the switch changes from off state to on state, current through the switch increases from 0 to a high value. Inductance components in the loop will limit the rate of current change and slow down switching speed.

Same as opening switch case, the loss consists of charging loss, switching loss and discharge loss. Higher off state impedance, lower on state impedance and faster speed will minimize energy loss.

When connected in parallel with the load, the closing switch can work as an element to stop energy delivery in a current source by current sharing. So it can be used in an inductive storage system to stop discharge.

Table 2.2 shows how all these switches can be used in a pulsed power system:

Table 2.2 *Typical applications of opening and closing switches*

Switch type	Connection method	Function
Opening switch	Parallel with load	Start inductive discharge
	Series with load	Stop capacitive discharge
Closing switch	Parallel with load	Stop inductive discharge
	Series with load	Start capacitive discharge

2.2.3 Pulse forming

Pulse is energy delivered in a limited period of time. Energy storage element works as a reservoir. The switch element controls the start and stop of energy delivery which will form pulses.

A pulse consists of 3 stages: rising edge (initiation of delivery), flat top (duration of delivery) and falling edge (stop of delivery). The pulse width is the sum of all these three. Comparing with the definition of pulsed power system, charging time should be longer than this pulse width.

Initiation of a pulse is controlled by a switch element as discussed in 2.2.1 and 2.2.2. Stopping of pulse can be controlled. Or the pulse will stop naturally when all the stored energy is consumed.

The load of a pulse forming system can be the storage element of an other system. This way, two systems are cascaded and higher peak power can be achieved.

2.3 Load and impedance matching subsystem

A Load in a pulsed power system will experience high power for a short period of time. High power/high voltage drives the load into nonlinear region. So its impedance may vary during the pulse. At the same time, the fast rise/fall time of the pulse implies a significant amount of energy is delivered as high frequency components. So parasitic inductance or capacitance may play an important or even dominant role in determining overall impedance.

And high power/high voltage of pulses may cause state change in the load not only electrically but also physically: a thin metal wire can evaporate in a pinch system; the medium can break down in gas discharge system like spark gap. So an impedance matching system should be carefully designed to maximize the energy delivery in most of the cases.

The hold off voltage of a single switch may be low. So output from several switches need to be added in order to get high voltage. This is also an output matching system, but in this case peak voltage or power is the major consideration not energy delivery.

Chapter 3 Circuit elements in pulsed power

As discussed in chapter 2, pulsed power system need circuit elements which can hold high voltage and have wide bandwidth. To hold high voltage requires large space to avoid unintended arcing, but wide bandwidth requires small geometry to minimize parasitic effect. Tradeoff between breakdown voltage and speed is a very important topic in pulsed power devices.

In this chapter, characteristics and performance of circuit components will be discussed and compared.

3.1 Storage elements

3.1.1 Capacitor

All capacitors are constructed by two metallic electrode plates separated by an insulating medium. Capacitors can be divided into 3 classes by the composition of the insulating medium and storage mechanism: electrostatic capacitor, electrolytic capacitor, and electrochemical capacitor.

Electrostatic capacitors use an insulating material between the metallic electrode plates as dielectric material. They have low capacitance values and are

non-polar. Examples of electrostatic capacitors include ceramic, Teflon, mica, and porcelain types.

Electrolytic capacitors use a solid or liquid electrolyte and have higher capacitance values than electrostatic capacitors. The dielectric layer in an electrolytic capacitor is formed by a very thin oxide on the metal plate surface. Two electrodes are the metal plate and the electrolyte. They are generally polar because a reverse-bias voltage will destroy the oxide material via electrochemical reduction. Electrolytic capacitors include solid and wet tantalum as well as aluminum types.

Electrochemical capacitors have a dielectric layer that forms naturally in the electrolyte with applied voltage. This dielectric forms in a very thin double layer on the surface of the capacitor's electrodes. Because of this effect, these capacitors are also known as double layer capacitors (DLC). The charge in these capacitors is not stored chemically but electrostatically.

The lumped circuit model of a 'real' capacitor is shown in Figure 3.1. The series resistor R_s is generally in the order of 0.1 Ω. It is due to the leads, the tab contacts, and the electrodes. The parallel resistance R_p represents the current leakage path through the dielectric and over the case material. The inductance L is associated with the internal arrangement of the capacitor which is a limiting factor on the peak current: $I_p = U(C/L)^{1/2}$. The capacitance and the leakage resistance depend on the temperature, voltage, humidity, working frequency and storage time.

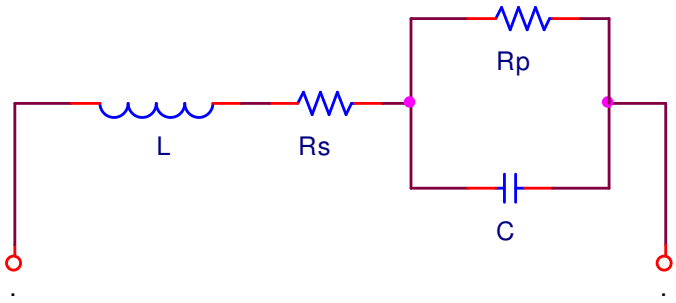

Figure 3.1 *Lumped element model of a capacitor*

Table 3.1 *Properties of different types of capacitors*

	Electrostatic capacitor	**Electrolytic capacitor**	**Electrochemical capacitor**
Dielectric material	Ceramic, plastic or other insulation materials	Metal oxide surface layer on electrodes	Dielectric double layer in electrolyte
Voltage rating	High	Medium	Low
Capacitance	Low	High	Very high
Energy density	Low	High	Very high
ESR	Low	High	High
Frequency dependence	Low	High	High
Temperature dependence	Good	Poor	Poor
Application	High speed high voltage stage	Low speed large energy bank	Low voltage large storage bank

Table 3.1 compares the major characteristics of different capacitors. The capacitor for pulsed power application is selected based on the following considerations. The high peak current associated with high power requires low series equivalent resistance. The wide bandwidth of the pulse power applications requires a stable capacitance value over a large frequency range. The hold off voltage of an electrostatic capacitor is propositional to the thickness of its dielectric layer and can

be easily extended by stacking. But the major disadvantage is the low energy density makes it not very efficiently in terms of spacing.

The energy stored in a capacitor can be calculated by $E=1/2CV^2$. For energy storage in a pulse power system, it will be wise to have a high voltage instead of large capacitance. The major reason is a large capacitor implies a large time constant for discharge which means slow speed.

So electrostatic capacitors with high voltage rating are most widely used in pulsed power systems. The electrolytic or electrochemical capacitors are only used as ac filter or low speed capacitor bank.

Among all types of electrostatic capacitors, metalized film capacitor and multilayer ceramic capacitors are most popular. The metalized film capacitor has a relatively small ESR and large energy density, which makes them useful in μs pulse applications. And many storage banks in the system are built by them. The ceramic capacitors has the fastest speed but less energy density and is mostly used in sub μs applications.

3.1.2 Inductor

An inductor is usually constructed as a coil of conducting material, typically copper wire, wrapped around a core of either air or ferromagnetic material. Figure 3.2 shows the lump element model of a real inductor. The major parasitic element is

equivalent series resistor Rs and equivalent parallel capacitor Cp. Rs characterizes the intrinsic loss of an inductor and Cp limits the maximum working frequency. For an air core inductor, the wire resistance is the major source of Rs which is called "copper loss". For a ferromagnetic core inductor (iron core inductor), eddy current on the surface of the core contributes to the loss as well which is called "iron loss". Cp comes from the capacitive coupling between windings and the capacitor formed by the winding and ground.

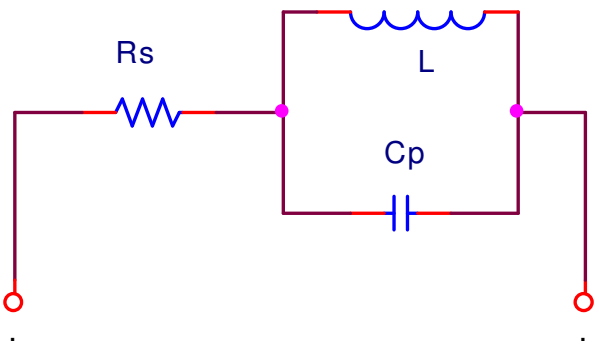

Figure 3.2 *Lumped element model of an inductor*

Table 3.2 *Electrical properties of air core and iron core inductors*

	Air core inductor	**Iron core inductor**
Inductance	Low	High
Energy density	Low	High
Working frequency	High	Low
Source of losses	Copper loss only	Copper loss and iron loss
DC ESR	High	Low
Frequency dependence	Weak	Strong
Low frequency performance	Good	Will saturate (core disappear)

Table 3.2 shows some difference between air core and iron core inductors. By using ferromagnetic material, the relative permeability can easily reach a few hundred to 10s of thousand. The inductance is propositional to the permeability so with same number of windings, the inductance for an iron core inductor can be much higher than air core one. This also means a larger energy density. But the permeability of the ferromagnetic material has a strong relation with frequency. This means the inductance can drop dramatically when frequency increases. And a more severe problem with iron core is saturation. Once the integration of voltage and time on an iron core reaches a certain value, the relative permeability of the core will drop to about 1. This can be seen as core “disappear” when a voltage applied on the inductor for a long time.

Because of this saturation problem, the storage inductor in a pulsed power system is normally an air core inductor.

3.1.3 Transmission line

A transmission line is constructed by two closely coupled conductors. The closely coupling means the most of the electric and magnetic field is confined in the space defined by two conductors. Figure 3.3 shows some typical transmission line structure and the lump element model of a lossless transmission line.

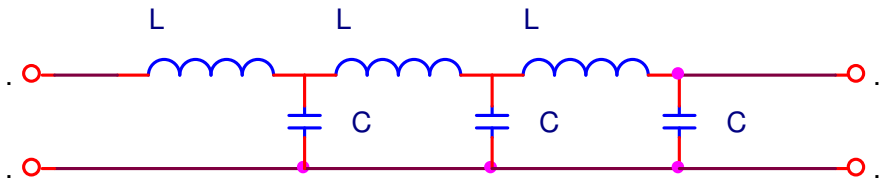

Figure 3.3 *Lumped element model of a lossless transmission line*

The transmission line model here has energy storage elements: inductors and capacitors which can be used to store energy. The energy can be stored in either electric field or magnetic field depending on the external circuit. If the transmission line is charged by a voltage source with the other end open, the energy is stored in the electric field between two conductors; if it is charged by a current source with the other end shorted, energy is in magnetic field. But normally, transmission line is used as a capacitive storage element. And the stored energy can be calculated by $E = \frac{1}{2} C_{total} V^2$. Here C_{total} is total capacitor of the transmission line which is the unit length capacitance multiplied by the length of the cable.

Two characters can be extracted from this lumped element model. One is called characteristic resistance $Z_0 = \sqrt{\frac{L}{C}}$ and the other is transmission delay T. T is like the time constant of transmission line, which determines the time need to discharge the line. And Z_0 is the transient impedance of the transmission line.

3.2 Solid state Switches

3.2.1 Thyristor

The thyristor is a four-layer semiconducting device, with each layer consisting of an alternately N-type or P-type material, for example P^+-N^--P-N^+. The main terminals, labeled anode and cathode, are across the full four layers, and the control terminal, called the gate, is attached to p-type material near to the cathode. The cross section of a thyristor is shown on Figure 3.4.

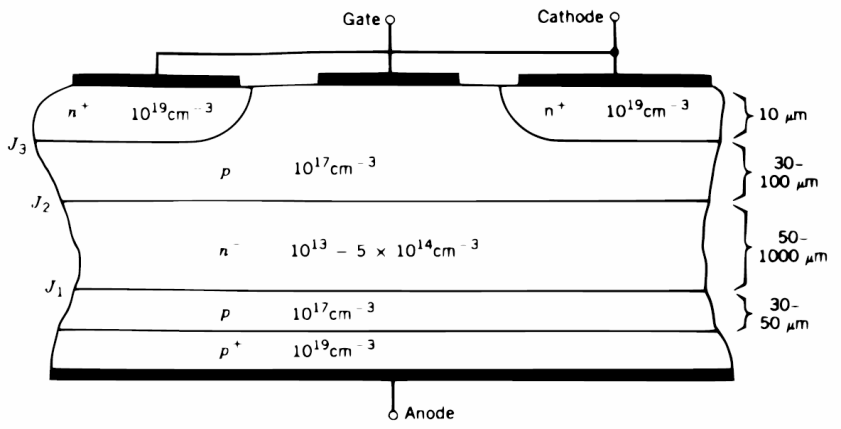

Figure 3.4 *Cross section of a typical thyristor*

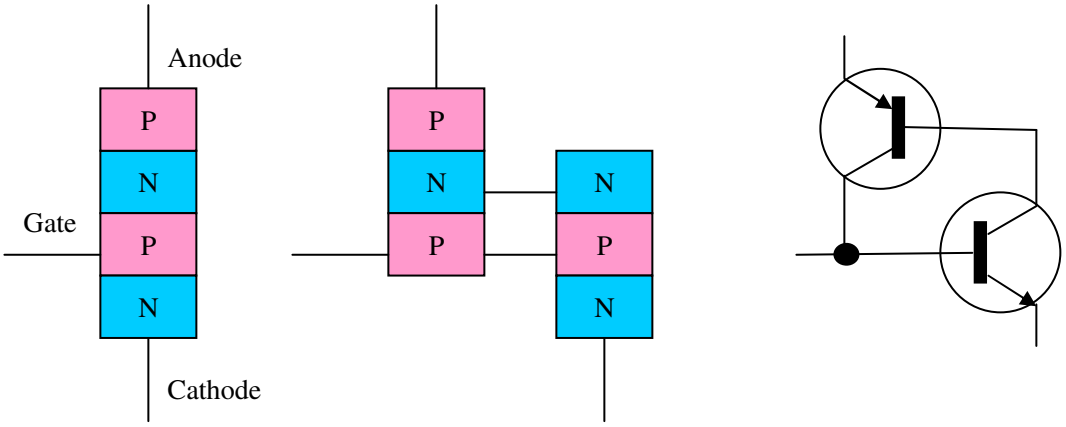

Figure 3.5 *Two-transistor equivalent circuit of thyristor*

Thyristors have the following three states:

1. Reverse blocking mode: Voltage on cathode is higher then anode. The two P-N junctions (P^+-N^- and P-N^+) is reversed and current flow is blocked. This also suggests that current can only flow in forward direction. Considering the doping profile, most of voltage will drop on P^+-N^- junction (J1) and which will determine the reverse hold off voltage.

2. Forward blocking mode: Voltage on anode is higher than cathode and the voltage difference on gate is low. In this case, the N^--P junction (J2) will block the current.

3. Forward conducting mode: Voltage on anode is high than cathode and a positive voltage is applied on gate. The positive gate voltage will cause avalanche breakdown of the N^--P junction (J2). This will bring the thyristor in conduction. The current through the device will maintain a positive gate voltage.

A thyristor operates in the following way: When the anode is connected to the positive voltage source, there is a reversed PN junction (J2) between gate and anode. Once a positive trigger is applied on the gate, electrons will be injected into gate from cathode. These electrons then travel into the space charge region of N^--P junction (J1) between gate and anode and collected by anode just like bipolar junction transistor. Or in other word, avalanche break down occurs in this junction.

The avalanche breakdown will be maintained by the positive voltage on the anode due to current flow.

If the interface of the gate contact is larger than that of the cathode, negative voltage on gate will cut off the current from cathode. And this device is a variant of thyristor which is called Gate Turn Off (GTO) thyristor.

State-of-the-art GTO thyristors can switch up to 6500 V and 4500 A. The pulses must be approximately 10 μs long, limited by carrier diffusion time. The devices can be stacked to increase the hold off voltage. They require no standby power and can switch large currents with a di/dt of nearly 10^{10} A/s. Limitations of thyristors include the long rise time, and they are susceptible to catastrophic failure under adverse circuit conditions. Thus, care must be taken in the design of the circuitry utilizing these devices, as any overvoltage or reverse bias can quickly lead to device failure.

3.2.2 MOSFET

The structure of the power MOSFET (metal oxide semiconductor field effect transistor) is shown in Figure 3.6. It has two terminals with same doping which is called source and drain respectively. Source and drain is separated by a channel with different doping. On top of this channel lays a conductor called gate which will control the conducting from source to drain. The gate is isolated from channel by a layer of oxide insulator.

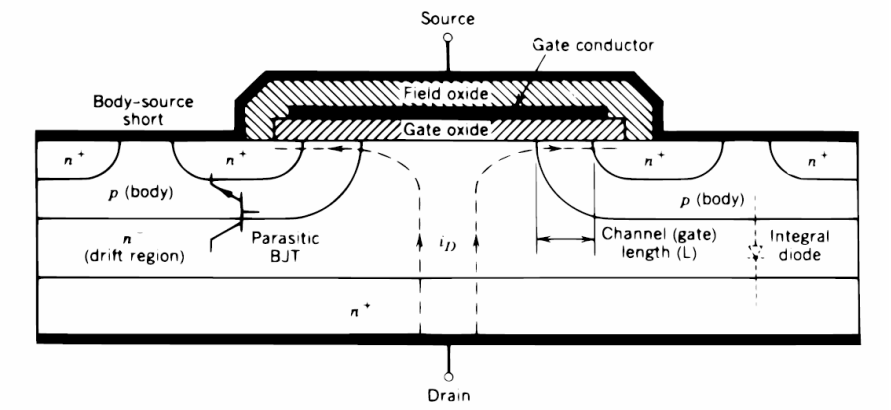

Figure 3.6 *Cross section of a typical power MOSFET*

As a switch, MOSFETs have 2 states:

Off state: Low voltage is applied on gate. Source and drain are separated by channel with different doping. The PN junctions block current flow between source and drain.

On state: A positive voltage is applied on gate. And a conductive channel is formed between source and drain which enables current flow.

The working principle of the MOSFET is that: a positive gate voltage will cause the formation of an inversion layer under the gate electrode. This inversion layer has same doping with drain and source, which will form a conducting channel between drain and source. So the device will be in on state. Removing charge on gate will destroy the inversion layer which will turn the device off.

The power MOSFET is voltage controlled, as the dc impedance of the gate-source path is practically infinite (10^9 Ω to 10^{11} Ω). It worth mentioning that during fast turn-on and turn-off the gate circuit does carry a short current pulse,

which is associated with the respective charging and discharging of the gate-source capacitance.

The velocity of the carriers in the channel is very high due to high source-drain voltage. So the carrier transition time will not limit the switching speed. The deterministic factor is the speed of adding or removing charge into gate. For MOSFET used in low voltage (drain-source voltage is comparable to gate threshold voltage), the charge needed to turn on the device is determined by the geometry capacitor constructed by gate and source. But in high voltage applications, parasitic capacitor between gate and drain (Miller capacitor) will play an important role in switching process. The large voltage change on drain will be fed back to gate by Miller capacitor. Thus more charge is needed to turn the device fully on. Although the Miller effect may slow the device down, a well-designed power MOSFET can have nanosecond switching time, which is much faster than thyrisitor.

Technical advantages of power MOSFETs are not limited to the high switching speeds. Little power is required to control them, and the control circuitry is much simpler than that for BJTs. The typical turn-on gate-source voltage is 20V, while a zero voltage is used to turn the device off.

MOSFETs have a negative temperature coefficient on drain current, which facilitates paralleling several transistors for an increased current handling capability. If the temperature of one of the component MOSFETs increases, the conducted

current drops, restoring the thermal balance among the connected devices. This characteristic also makes for uniform current density within the MOSFET, preventing second breakdown from occurring.

Voltage drops across conducting power MOSFETs can be as high as 10V, producing considerable conduction losses. On the other hand, the switching losses are low, even with high switching frequencies.

Single MOSFETs are available which can hold off 1200 V, while switching 120 A in pulsed mode. MOSFETs have larger conduction losses than IGBTs, especially at high load currents. MOSFETs are less prone to catastrophic failures than IGBTs, and thus require fewer external protection components. Their lifetime can exceed 10^{12} cycles. When operated in an avalanche mode, the rise time of these devices can be less than 1 ns.

3.2.3 IGBT

IGBT stands for insulated gate bipolar transistor. It is a FET controlled bipolar transistor. The cross section of a typical IGBT is shown on Figure 3.7. And the equivalent circuit of IGBT is shown on Figure 3.8. The IGBT has three terminals called Emitter (Source), Collector (Drain) and Gate. The structure is very similar to that of a vertically diffused MOSFET featuring a double diffusion of a p-type region and an n-type region. An inversion layer can be formed under the gate by applying

the correct voltage to the gate contact as with a MOSFET. The main difference is the use of a p^+ substrate layer for the drain. The effect is to change this into a bipolar device as this p-type region injects holes into the n-type drift region.

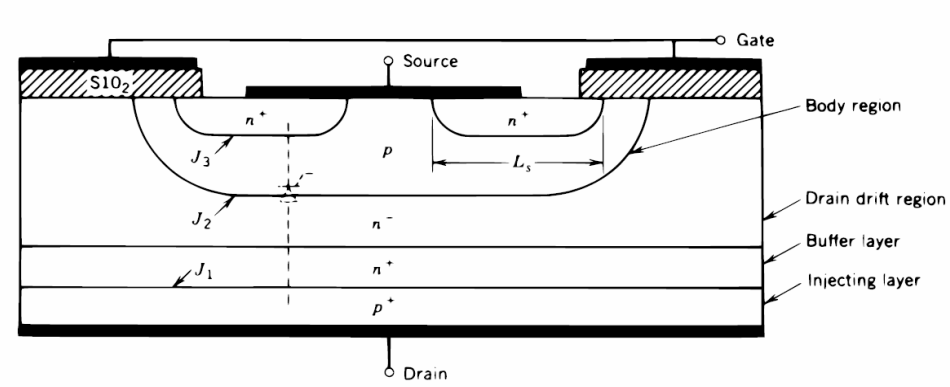

Figure 3.7 *Cross section of a typical IGBT*

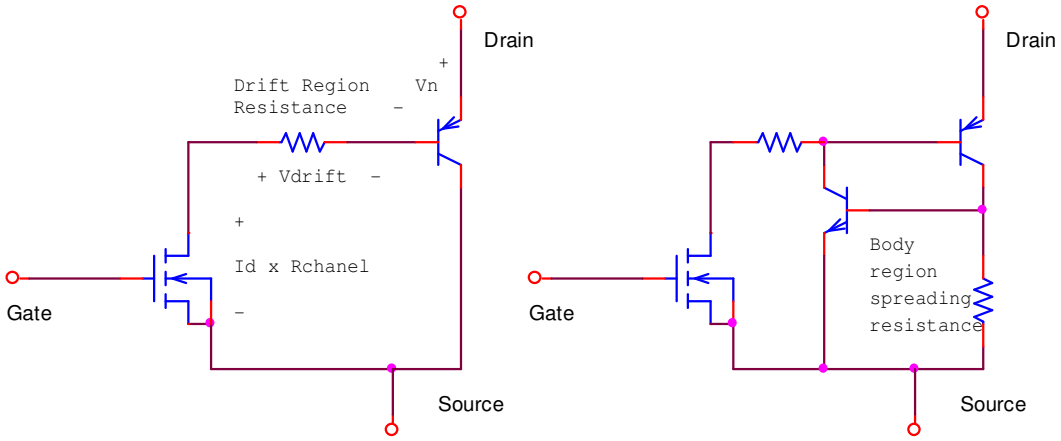

Figure 3.8 *Equivalent circuit of an IGBT*

As a switch element, it also has on and off states:

Off state: When gate voltage is low, current flow from drain to source will be blocked. Positive voltage is applied between drain and source. J2 is in reverse bias which blocks current flow, similar as MOSFET structure. So the hold off voltage is in same range of power MOSFET. If the voltage applied to the gate contact, with

respect to the emitter, is less than the threshold voltage V_{th} then no MOSFET inversion layer is created and the device is turned off. When this is the case, any applied forward voltage will fall across the reversed biased junction J2. The only current to flow will be a small leakage current. The forward breakdown voltage is therefore determined by the breakdown voltage of this junction.

On state: When a positive gate voltage applied, conducting channel appears under gate electrodes connecting source can drain drift region. This is electron conduction of IGBT. Source region is also connected to p type region which will work as collect in BJT. This is hole conduction. In Drain drift region, conduction is carried by both electrons and holes whose densities are several orders of magnitude higher than the original n^- doping. This will give a much lower on resistance then MOSFET which has only one type of carrier.

The turning on of the device is achieved by increasing the gate voltage V_G so that it is greater than the threshold voltage V_{th}. This results in an inversion layer forming under the gate which provides a channel linking the source to the drift region of the device. Electrons are then injected from the source into the drift region while at the same time forward biased junction J3 injects holes into the n^- doped drift region. The BJT can conduct much higher current than the MOSFET but it will take longer time to turn on the IGBT than MOSFET.

The Insulated Gate Bipolar Transistor is capable of switching 1700V and nearly 100 A over a single cell while using a very small gate drive of several volts and a few amps. The devices can be paralleled and stacked to some degree yielding modules capable of delivering very high currents to a load. The IGBT's simpler drive requirements, higher frequencies available (20 kHz), and its ability to generate arbitrary waveforms gives the IGBT a clear advantage over thyristors in nearly all applications, except those requiring extraordinary voltages and currents.

3.2.4 Magnetic switch (saturable inductor)

A practical magnetic switch is a device usually constructed as a winding around a magnetic core that uses the non-linear properties of magnetic material to achieve a large change in impedance. The inductance of this device is proportional to the relative permeability of the core. For ferri- or ferro-magnetic materials, the permeability is a function of the applied magnetic field. Permeability decreases dramatically when magnetic field approaching a certain value called *Hsat*(Saturation magnetic field). Figure 3.9 shows a magnetization curve (B-H loop) of a typical ferromagnetic material. The relative permeability is proportional to the slope of the B-H curve.

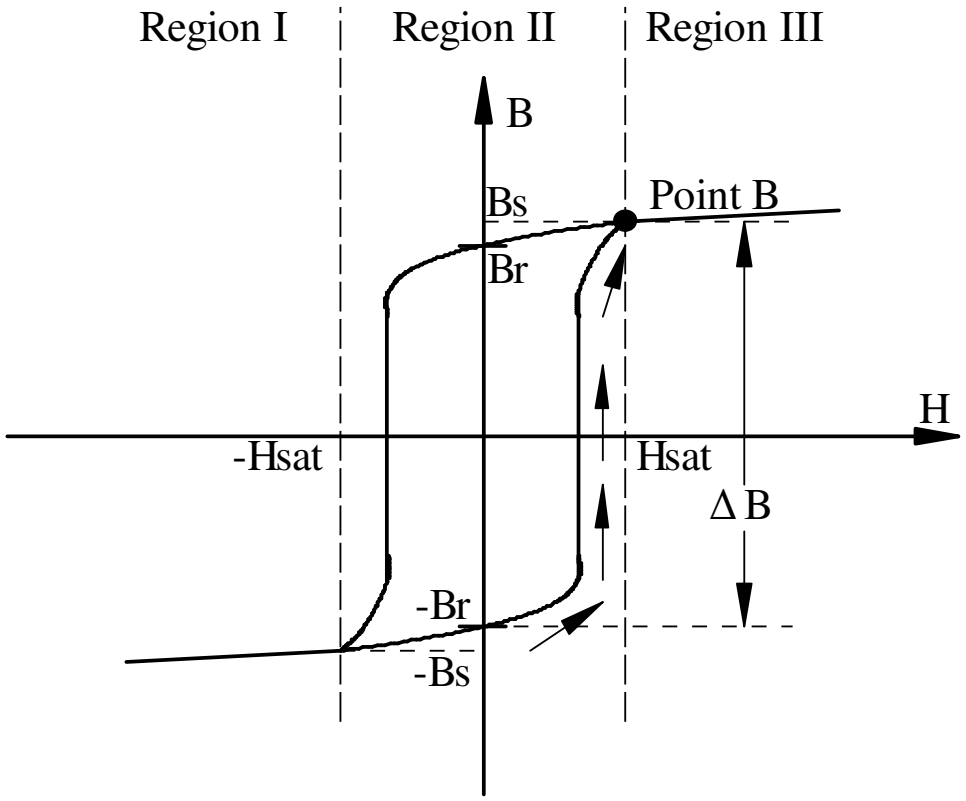

Figure 3.9 *Typical B-H curve of magnetic core in a magnetic switch*

There are clearly two states with large difference in permeability. In Region I and III, where *H* is higher then *Hsat*, the slope is about 1; In Region II, the slope is in the range of 100 to 10000. This phenomenon results from the alignment of the magnetic domain inside the material: when H is low, with the increasing of the magnetic field the domain will gradually align with the applied field and gives extra flux to the total magnetic flux density; if H is very high, all the domain will align with the field, so no further enhancement effect will take place. In this case, flux density *B* increases linearly with the ratio of μ_0 (permeability in vacuum).

These two states with large difference in permeability are corresponding to the on and off states of the switch:

Off state: The core is unstaturated so the relative permeability is very large. The inductance is very large which will prevent any change in current flow. The impedance of this device can be extracted : $Z_{off}=j\omega L_{off}$. Here $L_{off}=(\mu_0\mu_{rs}AN^2)/l$ is the off state impedance. The device has large impedance under high frequency, or in other word it blocks high frequency current.

On state: The core is saturated which makes relative permeability approximately 1. The impedance will lower by a factor of μ_{ru}/μ_{rs} The on state inductance is $L_{on}=(\mu_0\mu_{ru}AN^2)/l$.

The inductor switches from off state to on state once the current through the winding generates a high magnetic field excess H_{sat} of the core. The inductance of the device drops rapidly when H_{sat} increases which moves the device into on stae.

If a voltage V is applied across the switch, the switch will close at time t_{sat}, which is determined by : $\int_0^{t_{sat}} Vdt = N \cdot A \cdot \Delta B$, $\Delta B=B_{sat}+B_r$. Where μ_0, μ_{ru}, μ_{rs}, A, N, l, t_{sat}, ΔB, B_{sat} and B_r are permeability of vacuum, relative permeability of unsaturated state (normally a few thousands for ferri-magnetic material), relative permeability of saturated stare (close to 1), cross section of magnetic core, the number of windings, and the length of magnetic core, the time of core saturation,

flux density swing of the core, saturation flux density for the core and residual or remnant flux density in the core at the start of the pulse, respectively.

After switched on, the magnetic switch will remain on until the current drops below saturation value. So the magnetic switch can not be controlled to switch off.

The hold-off voltage of a magnetic switch is determined by the break down voltage between windings. The magnetic switch is normally an application specified designed. So the hold-off voltage, peak current and switching time can be quite different from device to device. Generally speaking, the maximum hold-off voltage for a magnetic switch is as high as 1000 kV and peak current is 100-1000 kA.

An important issue to make the switch stable over a long time is remnant flux density. The remnant flux density after every switching event can be different and it will accumulate over time. So the working point of the switch will gradually move to region I or III. According to the equation $\int_0^{t_{sat}} Vdt = N \cdot A \cdot \Delta B$, any change in B_r will change switch time t_{sat}. This will change the timing of this switch, makes it unable to precisely control turn on time. In the extreme case, once the working point is in regaion I or III, the device is unable to be in off state. To solve these problems, a core reset circuit is needed to bring B_r to a determined value.

3.2.5 Semiconductor Opening Switches (SOSs)

Semiconductor opening switch is a diode with special doping profile to enhance reverse recovery speed. Different from ordinary junction diodes, in these diodes the doping level is gradually decreased as the junction is approached. So a low doping region is formed between n^+ and p^+ regions.

A diode opening switch has three states:

1. Forward conducting: In this state, the voltage on anode (p^+ region) is higher than cathode (n^+ region). The diode is forward biased and current will flow through the diode. Charge is accumulated in the low doping region between anode and cathode.

2. Reverse conducting: In this state, reverse voltage is applied on the diode. But unlike ideal diode where the current will be interrupted immediately, reverse current will still flow from cathode to anode. This current provides electrons and hole to recombine with the carriers in low doping region.

3. Reverse blocking: In this state, space charge area is built up in the PN junction. Only a very small leakage current flows through the diode.

Current interruption in SOS depends on charge injected into the low doping n region of a p^+nn^+ structure. If the injection time is shorter than the lifetime of charge carriers in the material, amount of stored charge will equal to the charge carried by

forward current. The reverse current will deplete these accumulated charge carriers. Once all the carriers are recombined, the switch will not conduct any current.

To optimize the switch speed, several approaches are adapted. These results in three variations of opening switches: Step Recovery Diode (SRD), Drift Step Recovery Diode (DSRD) and Solid-state Opening Switch (SOS). SRD has a p^+nn^+ junction. The low doping n region can store more charges and give a higher current handling capability. A DSRD has an improved doping profile to optimize the distribution of the accumulated carriers. When pumped with a very short forward current, inhomogeneous electron-hole plasma will be created in the junction. This plasma can be depleted in a few nanoseconds by reverse current which gives ultra fast switching speed. In SOS, an additional low doping p region is introduced and a p^+pnn^+ junction is formed. This modification will increase the current handling capability of the device at the cost of switching speed.

A single solid opening switch can hold 1-1.5 kV which is similar to normal power diode. The switch can be stacked without any voltage dividers to achieve high hold-off voltage as large as 1 MV. SOSs can interrupt a current with a density up to 60 kA/cm^2 in less than 10 ns. DSRD has a lower current density capacity (100-200 A/cm^2) but a much faster switch time (0.5-1.5ns).

3.2.6 Summary

The properties of all the switches discussed in this chapter are summarized in Table 3.3. There is no "universal switch" good for all applications. An appropriate switch needs to be selected for specific applications to get best performance.

Table 3.3 *Comparison of typical solid state switches*

	Thyristor	**MOSFET**	**IGBT**	**Magnetic switch**	**SOS**
Hold off voltage	8.5 kV	1.4 kV	6.5 kV	1000kV	400 kV
Peak Current	1.2 kA	0.092kA	0.6 kA	100-100 kA	2kA
Rise time	>1000 ns	18 ns	270 ns	5-10000 ns	0.5 ns
Forward drop	2v	0.5 ohm	5v	-	-
Max repetition rate	10 kHz	3 MHz	100kHz	10 kHz	100 kHz
Trigger requirement	12v	15V	8-20V	No	No
Jitter	Small	Small	Small	Large	Small
Turn on cap.	Yes	Yes	Yes	Yes	No
Turn off cap.	No	Yes	Yes	No	Yes
Life time	10^8	10^8	10^8	10^8-10^9	10^8

3.3 Load

Same Load may perform quite differently in pulsed power condition comparing with low power operation. The I-V characteristic will be nonlinear at high power for various reasons. At high power, the load will heat up so the resistivity of the material will change accordingly. And at high voltage, dielectric breakdown will occur. When the duration of the pulse is shorter than the relaxation time, the load will be in

non-equilibrium state. In order to deliver energy efficiently to the load and get less distortion on the pulse, a careful analysis is needed. In this chapter, the characteristics of several loads used in our lab will be discussed.

3.3.1 Corona discharge load

A corona discharge load is constructed by a metal cylinder and a threaded rod or a gear in coaxial configuration. The cylinder works as cathode in discharge and the road/gear as anode. The volume enclosed by the cylinder is filled with gas/fuel mixture. Dimensions of the chamber are determined according to the specific applications. For a pulse detonation engine (PDE) tube, the inner diameter of the cathode is about 4 inches. A 10 mm diameter cylinder is used in internal combustion engine application.

When high voltage is applied on the discharge load, in the beginning it acts as a capacitor C_{geo} with capacitance determined by the coaxial geometry. Only displacement current flows through the load and charges this capacitor. Once the potential on anode reaches a threshold value, streamers start forming at the edge of anode and propagate towards the cathode. In this stage, the load can be modeled as C_{geo} in parallel with the series combination of $R_{streamer}$ and C_{var}. $R_{streamer}$ represents the resistance of streamer channels, which increases as the streamer front approaching cathode. C_{var} represents the capacitor formed by streamer front and

cathode which will also increase when the streamer head gets closer to the cathode. When streamer head reaches the cathode, C_{var} will disappear. Then, the impedance of this chamber is dominant by $R_{streamer}$. The streamer channels will be heated and grow wider. This will make $R_{streamer}$ decrease. One of these streamer channels may eventually develop into a highly conductive arc if the high voltage applies long enough. But if the high voltage is removed before arc formation, the streamer channels will get narrower and eventually disappear.

In ignition applications, energy needs to be delivered to the gas mixture in the chamber to initiate combustion. The low impedance of the arc makes it a poor candidate for energy delivery. So it will be more efficient if a pure streamer discharge is achieved.

There is no simple model to accurately describe this discharge process. The average value of $R_{streamer}$ is used to characterize the load which is about 100 to 200 Ohm. Since most of the energy is dissipated in the streamer channels, this simplification is proved to be reasonably good for design and analysis purposes.

3.3.2 Cuvette load

A standard electroporation cuvette is used to study the response of living cell upon nanosecond high electric field exposure. The cuvette is constructed by two 1 cm × 1 cm electrodes with 1mm gap. The electrodes are mounted on a plastic tube.

The volume defined by the plastic walls and electrodes is filled with nutrient solution in which the cells are suspended.

The water based solution has a resistivity of ρ ~500 Ω•cm. The dielectric constant of the solution is close to that of water $\varepsilon_r = 81$. The load behaves as a parallel combination of a resistor and a capacitor, with an RC time constant, $\tau=\rho\varepsilon_r\varepsilon_0$, of approximately 3 ns. The described cuvette with cell suspension in RPMI 1640 growth medium presents an electrical load of 11Ω in parallel with 55 pF. The impedance for a several nanosecond wide pulse is approximately 10Ω, which is used in the design of pulse generator for this load.

3.3.3 Catheter load

A microwave catheter consists of a coaxial cable and several discharge needles. The discharge needles are arranged like an extension of the coaxial structure. There is a center anode electrode and an array of cathode electrodes distributed evenly along the outer conductor of coaxial cable. The needle-like electrodes makes it easy pierce into tissues. When high voltage is applied, high electric field is generated in the volume defined by the needle electrodes. This way, high field can be delivered locally to any location of the tissue in a living animal.

The tissue is modeled based on its major composite which is salty water. The electrodes are arranged so that when all the electrodes are in the tissue the

characteristic impedance is close to 50 ohm in the frequency range of 10 MHz to 300 MHz. Several tests are conducted to verify this design and ~50 ohm impedance is achieved.

Chapter 4 Topology of the pulsed power circuit

In this chapter, typical pulsed power topologies are presented. These topologies are building blocks for a pulsed power system. These circuits can be used to drive not only a load but also other presented circuits. In other word, these basic circuits can be cascaded to gradually achieve the power and pulse width requirements.

4.1 RLC resonant circuit

RLC resonator is a fundamental circuit in pulse power system. It is widely used in pulse formation and analysis of other pulse power circuits.

A basic RLC resonant circuit is shown in Fig. 4.1. The circuit consists of two capacitor C_1 and C_2, an inductor L, a switch and a resistor R. C_1 is initially charged to voltage V and works as an energy source.

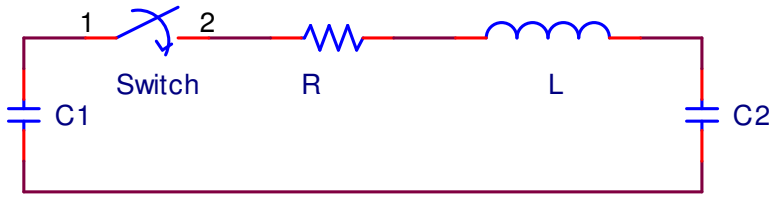

Figure 4.1 *Circuit diagram of a typical RLC resonant circuit*

The closing switch is used to isolate the source from the load. Once the switch closes, C_1 will discharge through R and L into C_2. This process is very important for pulsed power technique, so it will be analyzed in detail.

Considering energy preservation:

$$\frac{1}{2}C_1V_1^2+\frac{1}{2}LI^2+\int RI^2dt+\frac{1}{2}C_2V_2^2=\frac{1}{2}C_1V_0^2 \quad (4.1)$$

KVL:

$$V_1+L\frac{dI}{dt}+RI+V_2=0 \quad (4.2)$$

For C_1 and C_2, we have

$$I=C_1\frac{dV_1}{dt}=C_2\frac{dV_2}{dt} \quad (4.3)$$

d/dt of 4.2, we get

$$\frac{dV_1}{dt}+L\frac{d^2I}{dt^2}+R\frac{dI}{dt}+\frac{dV_2}{dt}=0 \quad (4.4)$$

$$L\frac{d^2I}{dt^2}+R\frac{dI}{dt}+I\left(\frac{1}{C_1}+\frac{1}{C_2}\right)=0 \quad (4.5)$$

Using the abbreviations:

$$\tau=\frac{L}{R},$$

$$C=\frac{C_1C_2}{C_1+C_2},$$

$$\omega_0^2=\frac{1}{LC},$$

$$\omega^2=\left|\omega_0^2-\frac{1}{(2\tau)^2}\right|,$$

We can rewrite (4.5) as

$$\frac{d^2I}{dt^2}+\frac{1}{\tau}\frac{dI}{dt}+\omega_0^2 I=0. \quad (4.6)$$

A solution of the differential equation (4.6) is obtained by using the ansatz $I = Ae^{\lambda t}$, with the initial condition *I(0)=0* and *dI/dt(0)=V₀/L*. For the characteristic roots $\lambda_{1,2}$, we obtain

$$\lambda_{1,2} = -\frac{1}{2\tau} \pm \sqrt{\frac{1}{4\tau^2} - \omega_0^2} \quad (4.7)$$

For further treatment we have to distinguish three cases:

1. $\omega_0\tau > 1/2$, this is under damped case.

$$I = \frac{V_0}{\omega L} e^{-t/2\tau} \sin \omega t \quad (4.8)$$

$$I_{\max} \approx \frac{V_0}{(L/C)^{1/2} + 0.8R} \quad (4.9)$$

In low loss situation, current gets its maximum value at $t \approx \frac{\pi}{2\omega} = \frac{\pi}{2}\sqrt{LC}$

In this case, the output voltage is

$$V_{C_2}(t) = \frac{V_0 C_1}{C_1 + C_2}\left[1 - e^{-t/2\tau}\left(\cos \omega t - \frac{1}{2\omega\tau}\sin \omega t\right)\right] \quad (4.10)$$

$$V_{C_2 MAX} = V_{C_2}\left(\frac{\pi}{\omega}\right) = \frac{V_0 C_1}{C_1 + C_2}\left(1 + e^{-\pi/2\omega\tau}\right) \quad (4.11)$$

(4.11) shows maximum energy transfer occurs at $t = \frac{\pi}{\omega}$. When loss is low (R is very small), $t \approx \frac{\pi}{\omega_0} = \pi\sqrt{LC}$.

The relative energy transfer ratio will be:

$$\eta = \frac{C_1 C_2}{(C_1 + C_2)^2}\left(1 + e^{-\pi/2\omega\tau}\right)^2 \quad (4.12)$$

The residual voltage on C_1 is

$$V_{C_1}(t) = \frac{V_0 C_1}{C_1 + C_2} + \frac{V_0 C_2}{C_1 + C_2}\left(\cos\omega t + \frac{1}{2\omega\tau}\sin\omega t\right)e^{-t/2\tau} \quad (4.13)$$

$$V_{C_1}(\max) = \frac{V_0}{C_1 + C_2}\left(C_1 - C_2 e^{-\pi/2\omega\tau}\right) \quad (4.14)$$

This case is mostly used in pulsed power systems Since the loss here will be low, it is used to transfer energy from two storage capacitors.

2. $\omega_0\tau = 1/2$. This is critically damped case.

$$I(t) = \frac{V_0}{L} t e^{-t/2\tau} \quad (4.15)$$

And the voltage on capacitor C_2 is

$$V_{C_2}(t) = \frac{V_0}{1 + C_2/C_1}\frac{1}{2\tau}\left[2\tau - (t + 2\tau)e^{-t/2\tau}\right] \quad (4.16)$$

3. $\omega_0\tau < 1/2$. This is over damped case

$$I(t) = \frac{V_0}{\omega L} e^{-t/2\tau}\sinh\omega t \quad (4.17)$$

The voltage on C_2 is

$$V_{C_2}(t) = \frac{V_0}{C_2\omega L}\frac{2\tau e^{-t/2\tau}\left(2e^{t/2\tau} - 2\omega\tau\cosh\omega t - \sinh\omega t\right)}{1 - 4\omega^2\tau^2} \quad (4.18)$$

Among all these three cases, under damped case is most widely used in pulsed power systems. One typical application is to transfer energy from one capacitor to another one. When the capacitances of these two capacitors are equal, all the storage

energy can be transferred in $t \approx \frac{\pi}{\omega_0} = \pi\sqrt{LC}$. Another application is energy conversion, where the stored energy can be transfer to the inductor *L*. In low loss condition, maximum energy transfer occurs when current *I* reaches $I_{\max} \approx \frac{V_0}{(L/C)^{1/2} + 0.8R}$ at $t \approx \frac{\pi}{2\omega} = \frac{\pi}{2}\sqrt{LC}$. If C_2 is much smaller than C_1, the peak voltage on C_2 will be twice the voltage on C_1. So, this configuration can be used to boost output voltage by a factor of 2.

A large potion of energy will be consumed by the resistor R in critically damped and over damped cases, which is useful when we want to deliver energy to a resistive load. In this case C_2 will not appear in the circuit, the pulse shape and peak amplitude can be calculated according to the formulas in the analysis. The critically damped is normally preferred, since the pulse duration $PW \approx 4.893\tau$ is shorter and amplitude $V_{\max} = 2V_0 e^{-1}$ is higher comparing with under damped case. This also means higher power. But this is hardly achievable in practices due to impedance change under high voltage or high power condition. It is normally works in slightly over damped region to avoid any oscillation.

4.2 Line type pulse forming circuit

The line type pulse forming circuit uses transmission line as storage and pulse forming element. The working principle is based on transmission line effect.

Any switching event can be seen as a wave traveling along the transmission line. A finite time interval is needed before the wave affecting the other end of the line, which is characterized by transmission line delay τ. Once the wave reaches the other end, part will transfer to the load and the other part will be reflected back. The reflection wave can be characterized by reflection coefficient:

$$\rho_V = -\rho_I = \frac{Z_{load} - Z_0}{Z_{load} + Z_0} \quad (4.19)$$

Here, ρ_v and ρ_i are voltage and current reflection coefficient respectively. Z_0 is the characteristic impedance of the line, Z_{load} is the impedance on the other side of the line.

There are many line type pulse forming circuits. Here we will use Blumlein circuit as an example to understand the working principle of line type structures.

A typical circuit diagram of Blumlein topology is shown on Fig. 4.2.

The transmission line is charged to V through R when S_1 opens. S_1 then closes which brings the voltage on this end down to 0. A negative going wave with amplitude of -V then travels along T_1 to load. After τ, -V wave see a $2Z_0$ load, a wave of –1/2V is reflected back towards S_1 along T_1, another –1/2V wave travels along T_2 away from load. Now a voltage V is established on the load. 2τ after S_1 closing , two –1/2V waves see the shorted switch S_1 and open end in T_2, and are reflected again. From switch end, a +1/2V wave travels along T_1 to the load and bring the voltage on

T_1 back to zero. From the open end of T_2, -1/2V is reflected and zeros the voltage on T_2. 3τ after S_1 closing, these two waves reach load again and cancel each other. The voltage on load then goes back to 0.

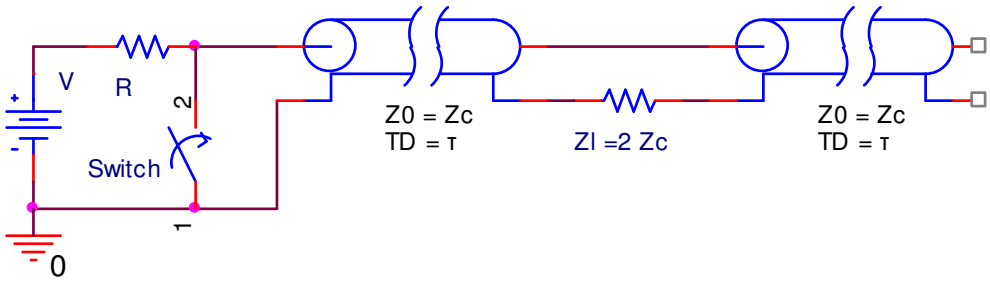

Figure 4.2 *A typical Blumlein line pulse generator*

The pulse generated by this Blumlein line circuit has amplitude of V and width of 2τ. The rise and fall time of the pulse is determined by the switching speed of closing switch S_1. There is an intrinsic delay of τ between closing of S_1 and appearance of V on load.

The Blumlein line circuit is easy to design and can deliver full charge voltage to the matched load. But as all other line type topology, a custom transmission line may be necessary for high voltage or special load impedance. And the wave shape is very sensitive to the load impedance.

Here listed a design flow chart of this Blumlein line circuit:

Step 1. Collect information: Load impedance Z_L, Output voltage V_{out}, Pulse width PW, Rise/Fall time t_r/t_f, repetition rate.

Step 2. Determine transmission line properties: characteristic impedance, $Z_0=Z_L/2$, break downvoltage $V_{br}>V_{out}$, delay $\tau=PW/2$.

Step 3. Build the transmission line.

Step 4. Test the transmission with low voltage pulses, determine the dispersion of the transmission line. Then find required switch rise time from t_r and t_f.

Step 5. According to the switch rise time, hold-off voltage V_{out}, max current V_{out}/Z_0, select a right switch. Leave some margin for max current (also affected by repetition rate)

Step 6. Determine trigger type according the switch type: over voltage for spark gap, gate trigger for IGBT/MOSFET.

Step 7. According to transmission line properties and repetition rate, determine the charging resistor value. Note that, an additional V/R will be added to the max current through the switch.

Step 8. Design the trigger circuit according to the switch requirement.

4.3 Marx bank circuit

A Marx bank circuit uses several (*N*) capacitors as energy storage element. All *N* capacitors are charged in parallel to V through resistors or inductors. After closing of the switches and these capacitors will be connected in series. Since the voltage across a capacitor will not change instantly, the N series connected capacitor (erected

capacitor) will have a voltage of *NV*. It will be delivered to the load. The pulse ends naturally when all the capacitor discharges or it can be ended by the opening of these switches.

Figure 4.3 shows a typical circuit diagram of Marx circuit. During charge phase, all switches are open and the voltage source charges all capacitor to V. Normally, there is a switch between the last capacitor and the load to isolate the load from charging source.

Once fully charged, the Marx circuit is ready to deliver pulses. Depending on the switch type, two slightly different processes will occur

a). Self-trigger system: Once the first switch closes, voltage across next switch will be 2V, which will trigger next switch. And this process continues towards the load.

b). Controlled trigger system: Every switch is controlled by an individual trigger. And these trigger signals are synchronized so that the switches will close at around the same time.

The "erected capacitor" C/N will discharge to the load with a time constant $\tau = R_{total} C / N$. Here the R_{total} is the load resistance plus the switch resistance. When full controllable switches are used, the output pulse width can be tuned by opening the switches. Otherwise, the fall time of the pulse will be determined by τ.

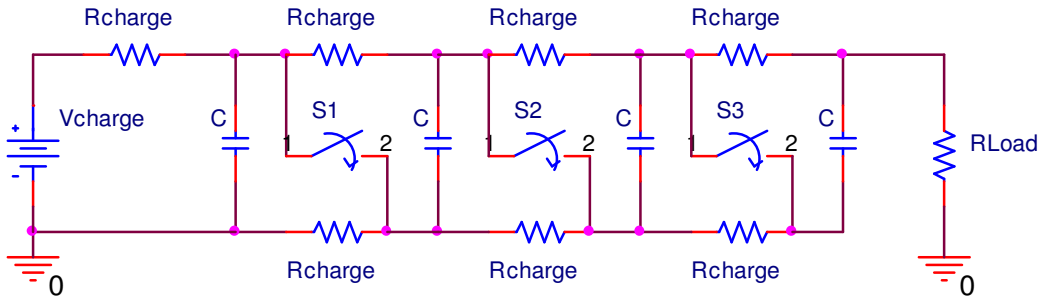

Figure 4.3 *Circuit diagram of a typical Marx generator*

The Marx circuit can generate pulses with amplitude of NV. The pulse width can be controlled. The rise and fall time are determined by the switch.

The Marx structure can be easily expanded by adding more stages. And the output voltage is not sensitive to load impedance. Full controllable switches are necessary in order to control the pulse width. Since both ends of the switches are floating above ground, the trigger signals are not referenced to ground.

And here is a design flowchart of Marx topology pulse generator:

Step 1. Collect information: Load impedance Z_L, Output voltage V_{out}, Pulse width PW, Rise/Fall time t_r/t_f, repetition rate.

Step 2. Determine switch type: If pulse width needs to be controlled or the output needs to be a square wave, full controllable switches should be used. Otherwise, self-triggered switches can be used to simplify the design.

Step 3. Determine the capacitor used in the system. Normally the capacitor should have an ESR much smaller than the total resistance.

Tunable PW design: the output in this case is normally a square wave. So the erected capacitor works as a capacitor bank. $\tau = \frac{C}{N}\left(R_{load} + NR_{switch}\right) > 10PW_{\max}$.

Fixed PW design: PW is normally dominant by the discharge process, so

$$PW \approx \frac{C}{N}\left(R_{load} + NR_{switch}\right)$$

Step 4. Determine number of stages N. The main consideration is the single switch hold-off voltage, power supply limit.

Step 5. Select the switches: Hold-off voltage $V_{hold}=V_{out}/N$; Current V_{out}/R_{load}; turn on time is less than rise time of the output pulse.

Step 6. Determine trigger type according the switch selection: over voltage for spark gap, synchronized gate trigger for IGBT/MOSFET.

Step 7. According to repetition rate, select appropriate value for the charging resistor. The energy should be restored during pulse interval.

4.4 Inductive adder circuit

Inductive adder is an output stacking technology. Instead of using 1:N transformer to step up voltage, N 1:1 transformers will be stacked to achieve voltage gain. The transformers isolate primary from secondary, so the secondary windings of these N transformers can be series connected to add the voltage. Comparing with 1:N transformer circuit, this adder scheme will cut the primary current by N at a cost of

increase the transformer number N times. This will also increase system complicity and total price. A typical circuit diagram shows in Fig. 4.4.

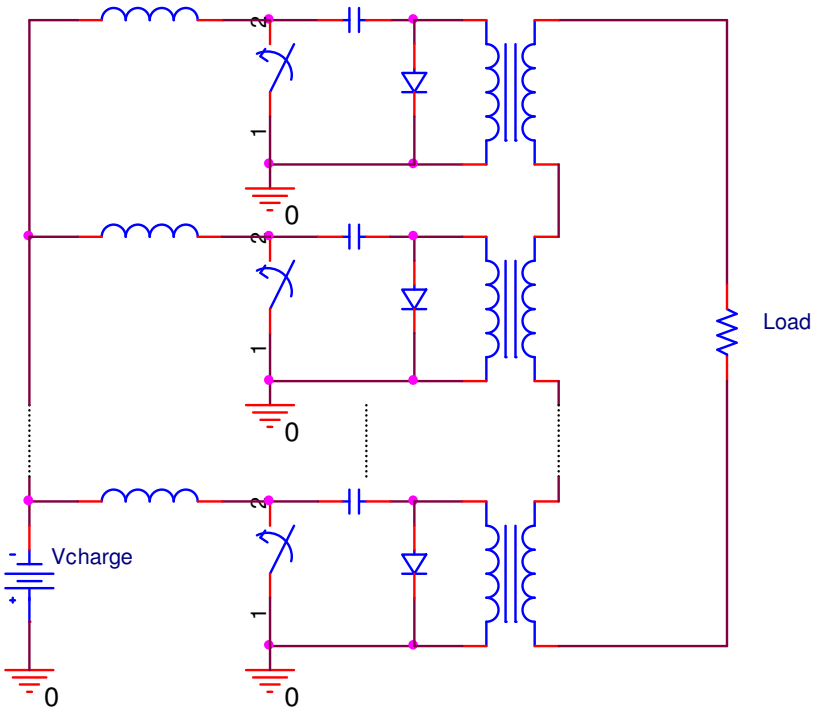

Figure 4.4 *Typical circuit diagram of an inductive adder*

The inductive adding circuit uses capacitive storage element $C_1 \sim C_N$. When switches are open, the capacitors will be charged to V. The closing of these switches enables current flow through primary winding which will generate voltage V on secondary for a 1:1 transformer. The secondary of transformer is not floating, so it can be connected in series and the voltage will add up. The output voltage is then NV. Here N is the number of transformers. Similar to Marx circuit, the pulse ends when all the capacitors are discharged or switches are turned off.

The inductive adder circuit can generate pulses with amplitude of *NV*. The width is controllable if full controllable switches are used which is similar to Marx circuit. One very important different comparing with Marx circuit is : all the switches are ground referenced. This makes the trigger circuit much simpler than Marx. The adder circuit can work with lower output voltage if some of the switches fail. The major disadvantage of this scheme is maximum pulse width is limited by saturation of transformer core. And the cores need to be reset to prevent accumulated magnetic flux density driving core into saturation.

The design of inductive adder is very similar to that of the Marx generator and will not be repeated here. Special attention needs to be paid to transformer design. In addition to traditional consideration like core saturation, coupling and etc, how the windings are wounded is very important. In order to get enough bandwidth to transfer fast pulse, the parasitic inductance of the transformer needs to be very small. For fast rise pulse, the number of windings in primary and secondary both limited to 1 or 2 turns. To magnetize the core uniformly, windings should be distributed evenly along the core. Evenly distributed parallel windings on primary and secondary are used to address this issue.

4.5 Magnetic compression circuit

Based on analysis of magnetic switch in chapter 3.2.4, a circuit can be build to compress a long voltage pulse. Figure 4.5 shows a basic circuit diagram of this compression scheme. The circuit consists of 2 capacitors C_1 and C_2 which are connected by a magnetic switch L. Based on the analysis in chapter 4.1, in order to get maximum energy transfer, C_1 and C_2 should have same capacitance.

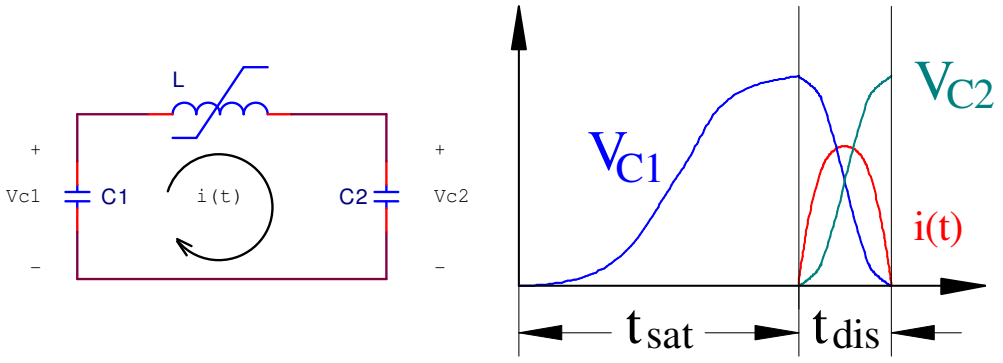

Figure 4.5 *One stage of typical magnetic compression circuit*

C_1 and C_2 are initially discharged, so the voltage difference across L is 0. L is in unsaturated state and has large inductance. The large inductance implies current blocking function of the switch L. Assuming C_1 is charged by a RLC circuit (which can be a similar compression circuit). According to the analysis of under damped circuit in chapter 4.1, voltage on C_1 will also increase according to equation (4.10). Then, a voltage difference will build up on L. Current flows through L will increase

accordingly: $I = \frac{1}{L_{unsat}} \int (V_{C_1} - V_{C_2}) dt$. When the voltage on C_1 reaches its peak value V_p, all energy is transferred to C_1. It is time for magnetic switch L to turn on. According to (3.1), we get

$t_{sat}=2\ N\Delta B\ A/V_p$ (4.20)

Once L saturated, the inductance will drop to L_{sat}. C_1, L_{sat} and C_2 form a RLC resonant circuit. Energy will transfer from C_1 to C_2 through $L_{sat.}$

Let the capacitance of C_1 and C_2 be C. The charge in C_1 will fully transfer to C_2 after t_{dis}.

$$t_{dis=} \pi \sqrt{L_{sat} C / 2} \quad (4.21)$$

This way, a pulse with rising time t_{sat} will be compressed into t_{dis} and gives a compression ratio of:

$$Gain=t_{sat}/t_{dis} \qquad (4.22)$$

Magnetic switches have a very long lifetime, as they do not suffer from erosion problems like gas switches. They can be operated at high repetition rates (1kHz and above). And they are reliable and rugged. The disadvantages of this circuit are: 1. Heat generate by the core loss will change the core properties which will lead to drift in t_{sat}. 2. The core material will be very lossy at high frequency which make short pulse (<100ns) can not be compressed efficiently. 3. Remnant flux may accumulate over a long period of time (several days or even weeks) which will eventually lead to

unexpected saturation of the core. So a reset circuit is needed for stable operation of magnetic switch.

And here is a design flowchart of Magnetic compression circuit:

Step 1. Collect information: Load impedance R_L, Output voltage V_{out}, Pulse width PW.

Step 2. Select core material according to pulse width. The material should have a wider bandwidth than the pulse.

Step 3. Determine saturated inductance $L_{N\text{-}sat}$, storage capacitor C and charge voltage on C according to PW, V_{out} and R_L. Using equation for critically damped case, $PW \approx 4.893\tau = 4.893\frac{L_{N-sat}}{R_L}$. $C = 4\frac{L_{N-sat}}{R_L^{\ 2}}$ $V_{out} = 2V_{charge}e^{-1}$

Step 4. Select core shape and size and determine number of winding. Normally a toroid core is used. Use equation $L_{sat} = \frac{\mu_0 \mu_{r-sat} N^2 A}{2\pi R}$ select core size and number of windings. Here $\mu_{r\text{-}sat}$ is the relative permeability of the saturated core, N is the number of windings, A is the cross-sectional area of the core, R is the toroid radius to centerline. The solution of this equation is not unique. Some other constrains, such as availability of the core material, spacing for insulation between windings, need to be considered to ensure that the inductor can be made.

Step 5. Calculate t_{sat} using V_{charge}, N, A. Determine if an additional compression stage is needed.

Step 6. Go back to Step 3 to design additional compression stage (stage number N-1) if it is necessary.

4.6 Diode opening switch circuit

Diode opening switch (DOS) have extremely fast recovery time and high current handling capability. It can be used in inductive storage system. According to the analysis in chapter 3.2.5, the following 3 steps are required in order to use a DOS.

Forward pumping: Current flows from anode of the DOS to cathode. Electron-hole plasma is built in PN junction, which can be seen as charge stored in a capacitor.

Reverse pumping: Current flow from cathode to anode. Electron-hole plasma is gradually depleted. Current flows in this phase will charge an inductive storage element. The inductor will deliver stored energy to a load once DOS switches off.

Reverse recovery: After electron-hole plasma depleted, no carriers appear in the junction area. The current will be interrupted abruptly. Current interrupting speed depends on the diminishing of electron-hole plasma which is directly related to the reverse and forward pumping.

Figure 4.6 shows a typical pulse sharpening stage using DOS. In the first half cycle, S1 is open and the diode is forward biased and current flows (red curve) from

ground to the capacitor and charge the capacitor C. Once the capacitor is fully charged, S1 will close and C1 will discharge through the inductor L (current flows along the blue curve). Reverse current will flow in the diode. After all the charges are recombined, the diode suddenly changes to current blocking state, resulting in a fast current interruption. In order to get maximum energy delivery into load R, the DOS should switch when the current in the inductor is maximized (thus all the energy transfer to the inductor). After the current switched to the load, it will decays according the L/R time constant. This will be the falling edge of the output pulse on R.

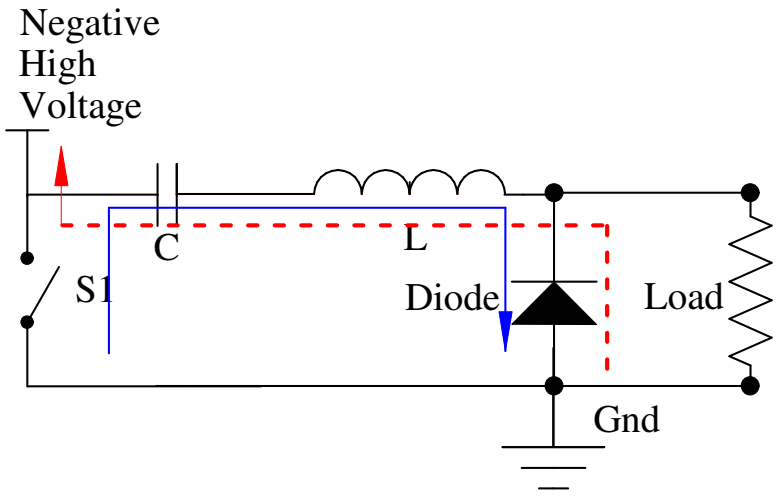

Figure 4.6 *Typical SOS based pulse compression circuit*

Comparing with other solid state opening switches like IGBT, MOSFET, DOS can handle a large current density in nanosecond or sub-nanosecond range. Or in other word, DOS is the only solid state opening switch which can interrupt >100 A

current in nanosecond range and hold kV range voltage. The main disadvantages for the DOS technology are: 1. Forward pumping time of ~100 ns is normally needed for nanosecond range switching. So the SOS can not be used to compress long pulses. 2. The DOS circuit is an inductive storage circuit so the output voltage depends on load impedance.

4.7 Summary

Table 4.1 lists the performance of all pulse forming topologies discussed in this chapter for comparison.

Table 4.1 *Performance of different pulse forming topologies*

	Blumlein	**Marx**	**MPC**	**Adder**	**DOS**
Pulse amplitude	V_{charge}	$N\ V_{charge}$	$\sim 0.7\ V_{charge}$	$N\ V_{charge}$	$R_L I_{charge}$
Pulse width	2τ (line delay)	Controlled by trigger	~2L/R_{load}	Controlled by trigger	~2L/R_{load}
Pulse rise time	Switch speed	Switch speed	$\sim (LC)^{1/2}$	Limited by leakage inductance	Switch speed
Pulse fall time	Switch speed	Switch speed	$\sim L/R_{load}$	Switch speed	$\sim L/R_{load}$
Delay	Line delay	Switch delay	Core saturation time	Switch delay	Forward pumping time
Repetition rate	*1/(PW+charging time)*	*1/(PW+charging time)*	*1/(PW+charging time+core reset time)*	*1/(PW+charging time+core reset time)*	*1/(PW+forward puming+Revers e pumping)*
Switch current	$2V_{charge}/R_L$	$N\ V_{charge}/R_L$	$V_{charge}/(R_L \times$ *compression ration)*	$N\ V_{charge}/R_L$	I_{charge}

In this table, V_{charge} and I_{charge} represent charging voltage and charging current, R_L is load impedance. N is number of stages in adding circuits. PW is pulse width.

Chapter 5 Pulse generator for biological and medical applications

Electric fields control transport processes across membranes and play an important role in biological systems. A dielectric membrane formed by a 5 nm thick insulating phospholipids double layer separates internal structures of a cell (cell nucleus, organelles, and cytoplasm) from the exterior. The membrane has high breakdown strength ($2x10^6$ V/cm, or 1 V membrane potential). Short time exposure to high voltage will create some small holes (pores) in the membrane temporarily and increase the permeability of the membrane.

The cytoplasm is an electrolytic conductor and electric field applied will move ions in cytoplasm. The cell becomes polarized, which will screen the interior structure from the applied field after a short transition period.

The relaxation time τ for complete polarization depends on the cell dimensions, the specific membrane capacitance and the conductivities of the cytoplasm and the suspension:

$$\tau = aC\left[\rho_i + \frac{\rho_e}{2}\left(\frac{1+2f}{1-f}\right)\right] \quad (5.1)$$

τ is the relaxation time constant, C the capacitance per unit area, ρ_i is the resistivity of the cytoplasm, ρ_e is the resistivity of the suspension and f is the volume

fraction of the suspension occupied by cells. τ is from 10s of nanosecond to a few hundred nanosecond depends on the cell species.

Short (10s of nanosecond) pulses can either non-destructively create pores on cell or directly affect interior structures of cells. This makes it very interesting to study the cell response after exposed to such short pulses.

5.1 Design goal

At this moment, most pulsed power systems for studying nano-electroperturbation are developed in two research laboratories at University of Southern California and Old Dominion University. Most pulse generators used in cuvette experiment is based on gas switches (spark gap). The output pulse width and amplitude are 5-20 ns and 1-10 kV respectively. Because of erosion, the spark gap needs to be tuned after running for certain period of time. And an exposed spark gap switch is very sensitive to surround gas and moisture.

To improve the stability and minimize the pulse generator, it is worthwhile to build a pulse generator with full solid state components. The full stolid-state system has theoretically infinite lifetime and once it is tuned no further adjustment is necessary during operation. By changing the charging voltage on storage capacitor,

output amplitude can be varied in a certain range without much change in pulse duration.

A full solid-state pulse generator based on diode opening switch is implemented by Dr. Kuthi at USC Pulsed Power Lab for microscopic electroperturbation experiment. That pulse generator is design to work with a 50 Ω 100 μm microchamber load thus the output current and voltage is only about 20 A and 900V respectively. A standard cuvette load has 10 Ω impedance and 1 mm spacing. For this load, an output pulse of 5 ns 10 kV and 1kA is preferred for electroperturbation study.

5.2 Magna-I 20ns 3kV pulse generator

The circuit diagram of the 20 ns pulse generator is shown in Figure 5.1(a). The system consists of 3 functionally distinct stages: an LC resonant charge stage, a magnetic pulse compression stage, and a diode opening switch stage. In the design, pulses generated in LC resonant stage (3 kV, 1 μs) are compressed to ≈180 ns by a saturable inductor L_1. A saturable transformer T_2 transfers these 180 ns pulses through the forward conducting diode into a storage capacitor C_2. The transformer then saturates, and a 560A, 90ns reverse current pulse flows through the diodes. At the moment reverse current reaches peak value, the diode will turn off and block current flow. Then the current will be delivered to the load. A 4.5 kV amplitude, 20

ns wide pulse then appears on the load. A picture of the pulse generator is shown in Figure 5.1(b).

The stage-by-stage design starts from calculating pulse parameters at the load and working back to the LC resonant stage, which will be presented in the following chapters.

(a)

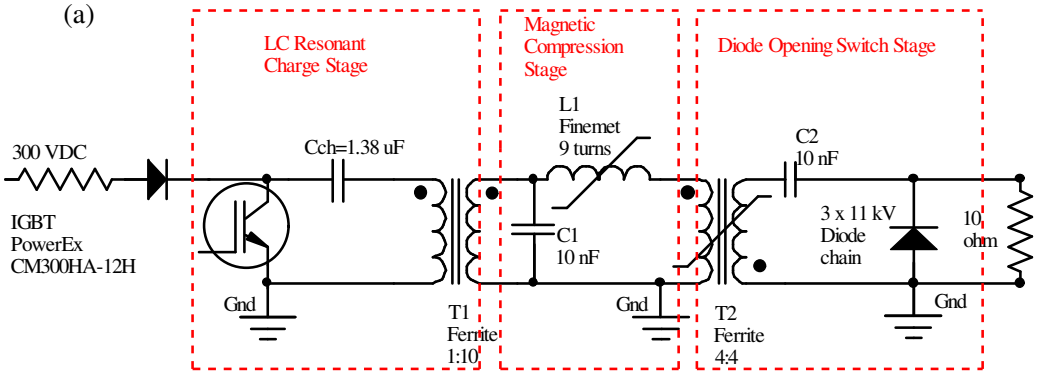

(b)

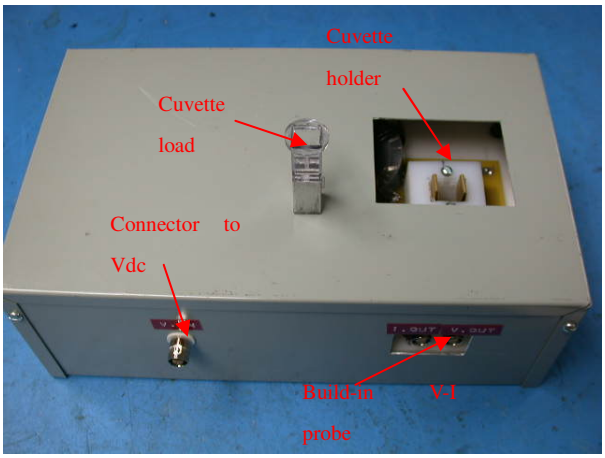

Figure 5.1 *(a) Circuit diagram of Magna-I pulse generator. (b) photo of Magna-I pulse generator with a cuvette load.*

5.2.1 Load analysis

The load is a standard electroporation cuvette as discussed in chapter 3.3.2. At the operation frequency of the pulse generator, the load impedance Z_L is about 10 Ω. In order to generate a 5 ~ 10 MV/m electric field in the chamber, pulses with 5 ~ 10 kV in amplitude are required. Accordingly, the output current will be 500 ~ 1kA. Considering a pulse width of 5 ns, energy delivered per pulse is approximately 50 mJ.

5.2.2 Diode opening switch

Instead of optimized diode switch with special doping profile, mass manufactured MURS2510 automotive rectifiers (1 kV, 25 A, dc rating) are used in the design reported here. Comparing with special diode, this type of diode needs a very short forward pumping in order to turn off rapidly. When this diode is fully saturated by forward current, it will suffer a long reverse recovery time. Here the reverse recovery time is defined as the period of time when reverse current flows before diode turns off. For a fully saturated P/N junction, the reverse recovery time is normally in hundreds of nanoseconds range, which will make the output pulse width significantly longer.

An important characteristic of a diode working as nanosecond opening switch is maximum forward pumping time, which is defined as the longest diode forward

conducting time without fully saturating the diode. It indicates the longest pulse which the diode can compress efficiently. The larger this value is, the faster the diode can switch. This value is about 200 ns for a single MURS2510 diode. In order to hold 10 kV, eleven diodes is connected in series. Three diode chains like this are connected in parallel to meet the current requirement. This parallel combination also reduces pre-pulse pedestal caused by the resistive phase during the forward pumping time. The series-parallel connected diode block shows degradation in switching speed compared with a single diode. The maximum forward pumping time drops to about 100 ns for a single chain, presumably because of the diode capacitance reduction.

The actual current through diode is shown in Figure 5.2. The amplitude of the current is close to the designed value and the pumping time is slightly longer. A possible reason is parasitic inductance. This increase in pumping time results in lower output amplitude and larger pulse width.

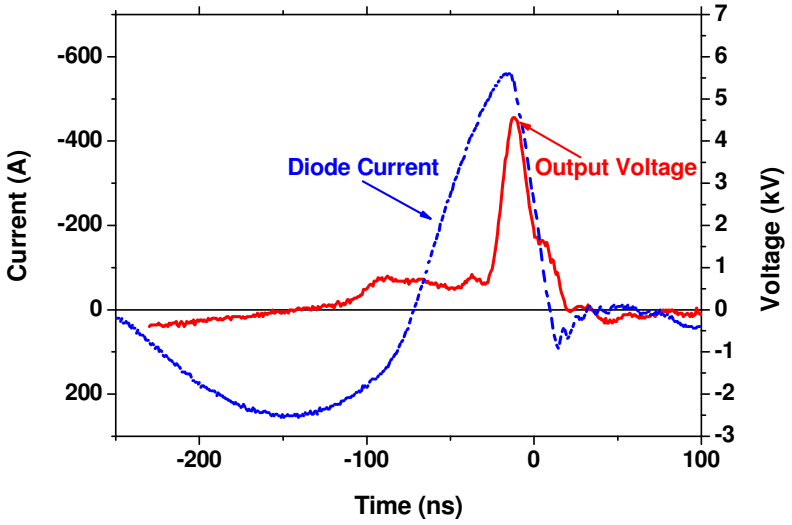

Figure 5.2 *Current through diode D and voltage cross D in Magna-I pulse generator*

The working principle of this diode opening switch circuit is illustrated in Figure 5.3. The pulse generating cycle begins with switch S_2 closed and S_1 open, so the first capacitor is fully charged and the second is empty. Then switch S_2 opens and the subsequent closing of switch S_1 generates a half cycle of forward current through the diode. This establishes stored charge in the diode depletion layer and transfers the initial charge from the first to the second capacitor. At the end of this half period the second switch S_2 closes and starts a reverse current through the diode depleting the stored charge. In an ideal circuit with ideal switches and lossless circuit elements the two capacitors and the two inductors must be equal. For constant capacitor voltage, the peak inductor current is proportional to the circuit admittance, $I \propto \sqrt{C/L}$. During the forward current phase the total circuit inductance is 2L and the net

capacitance is C/2. During the reverse current phase the net inductance is only L and the net capacitance is C. Both phases have the same resonant frequency. Thus the peak reverse current will be twice the peak forward current, and the charge will be extracted at exactly a quarter period, at the peak of the reverse current. The opening of the switch S_1 recharges the first capacitor and completes the cycle.

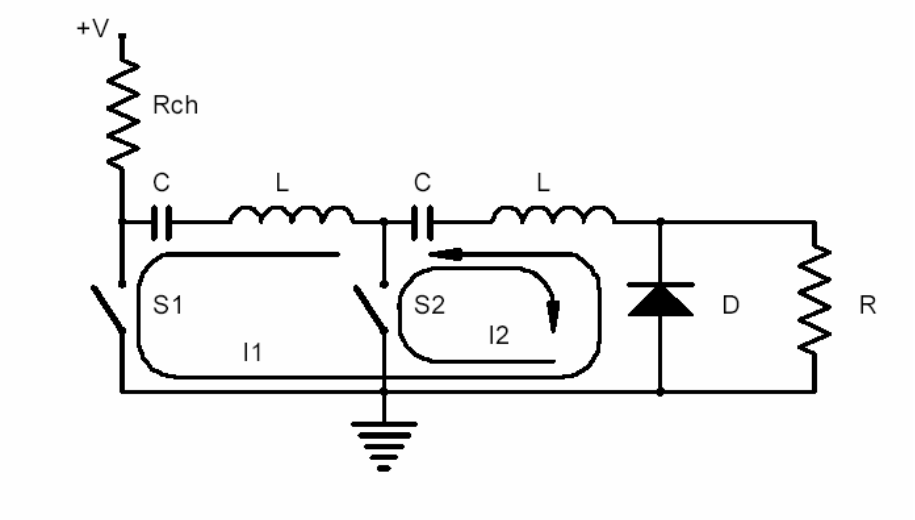

Figure 5.3 *Principle of diode opening switch sharpener*

5.2.3 Saturable transformer

The energy delivered to the load comes from that stored in the inductor formed by the secondary winding of a saturated transformer T_2. According to the current and energy values calculated in 5.2.2, inductance of the saturated secondary should be 400 nH (L_{sat2}).

The saturable transformer generates the forward and reverse pumping required by the diode stage. As analyzed in 5.2.2, the saturable transformer has a compression

ratio of 2. So diode reverse conducting time is ~90 ns, which is also a quarter period of the L_{sat2}, C_2 resonant circuit. Based on this, the final storage capacitance C_2 needs to be 10 nF and the peak charging voltage across C_2 is ~3 kV.

The transformer is wound on a CMD5005 ferrite core from Ceramic Magnetics. According to the datasheet, the core will work over a wide frequency range up to ≈100 MHz. The dimensions of the core are OD = 50.8 mm, ID = 25.4 mm, H = 12.7 mm. The core saturates at B_{sat} = 0.33 T. The saturated permeability is ~4. In order to obtain L_{sat2} = 400 nH, 5 turns for the secondary winding is needed. The primary winding is also 5 turns, since a 1:1 turn ratio is required.

In actual circuit construction, the leakage inductance of the transformer contributes to the total inductance as well as the parasitic inductance of the diode chain and the PCB trace. So the primary and secondary windings are wound as adjacent to each other in order to reduce leakage inductance. The actual number of turns was reduced to 4:4 for best performance.

Figure 5.2 shows experimental data for a forward pumping time of 182 ns and a reverse pumping time of 58 ns. The peak forward and reverse current are 256 A and 560 A, respectively, which is close to the design value. The difference is caused by parasitic circuit elements, mostly inductance, and timing shifts introduced by core bias shifts.

5.2.4 Magnetic compression

The output of the magnetic compression stage feeds into the primary of the saturable transformer T_2. So the output pulse of this stage should have a width of 140 ns and amplitude of 3 kV.

Since the saturable transformer has a 1:1 turn ratio, the capacitor C_1 in the magnetic compression stage should have same capacitance with C_2 for maximum energy transfer. C_1 discharges through the saturable inductor L_1 into C_2 through transformer T_2. The charge transfer time is a half period of the LC series resonant circuit ($\pi\sqrt{L_1 \cdot C_1 \cdot C_2/(C_1 + C_2)}$), which is also the forward pumping time (180 ns) of the diode stage. This determines the series-combined transformer leakage inductance and saturated inductance of L_1. This total inductance can be inferred from the current waveform in Figure 5.2, to be ~700 nH.

To achieve a high compression ratio, a core with large saturation magnetic flux density (B_{sat}) is preferred. Finemet core from MK-Magnetics is chosen for its large Bsat (1.23 T) and high working frequency. The external dimension of the core is OD = 50.8 mm, ID = 25.4 mm, H = 12.7 mm. Calculation suggests 7 turns on the core for correct forward pumping. With 7-turn winding, the inductor will saturate in about 1.3 μs, which is the minimum charge transfer time for the L-C resonant stage.

During construction of the pulse generator, it was found that the inductor L_1 saturated early with 7 turns. There are two ways to solve this problem: increasing the effective B_{sat} by biasing the core to the opposite direction of saturation; or increasing number of turns. To simplify the design, the second method was adopted and 2 more turns was added to the winding. The compression stage compresses 1 μs pulse into 180 ns, which gives a compression ratio of about 5.

5.2.5 LC resonant charging

An L-C resonant stage is used to generate pulses on C_1 required by magnetic compression stage. The main dc power supply voltage is 300 V, which suggests the adoption of a 1:10 ratio step-up transformer to raise the voltage to the required 3 kV across C_1. The transformer will match the effective capacitance of primary to secondary to get maximum energy transfer, which gives for the primary capacitor a value of C_{ch} = 1 μF. Considering the losses in the transfer, a slightly large value (1.38 μF) was selected. The leakage inductance of the transformer dominates the total inductance, and determines the pulse width. By trial and error, an actual number of 1:10 was found to meet the timing requirement. Based on the previous data, the switch on the primary side needs to hold 300 V and handle a peak current of about 600 A. To fulfill the specification, an IGBT (CM300HA-12H) from PowerEx is selected.

5.2.6 Testing

Magna-I is tested with using a standard cuvette filling with RPMI nutritious media without cell. A repetition rate of 20 Hz is achieved. Typical output into a cuvette load with 85 µl RPMI is shown in Figure 5.4 (a). The pulse amplitude is 4.56 kV, and the FWHM is 18.4 ns.

By varying the charging voltage, different output amplitudes can be achieved. In Figure 5.4 (b), the effect of charging voltage on the output pulse is shown. This also called "control curve" of the Magna-I. According to this control curve, the output amplitude can be tuned from 5 kV to 3.5 kV with a relatively fixed pulse width ~20 ns. The pulse width will increase dramatically when the charging voltage is less than 250 V. The reason may be because the incorrect saturation time of L_1 at low voltage.

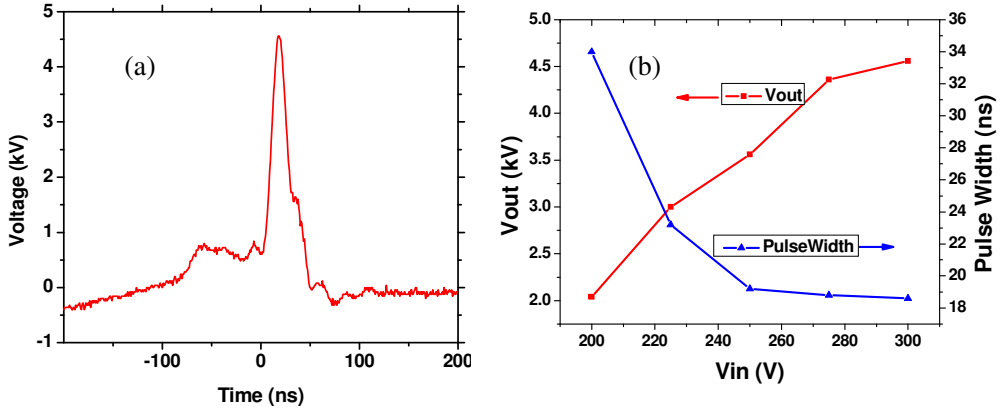

Figure 5.4 *(a) Output pulse of Magna-I with cuvette load, (b) Output pulse amplitude and width vs different charging voltage in Magna-I*

5.3 Magna-II 5ns 7.5kV pulse generator

Magna-I covers the range of electric fields up to 4.5 MV/m and can only give pulses of about 20 ns and 4.5 kV for 10 Ω cuvette load. The design is modified in several aspects in order to produce shorter and larger amplitude pulses. Figure 5.5 (a) shows the circuit diagram of the modified pulse generator. The photo of the constructed pulse generator is shown in Figure 5.5 (b).

(a)

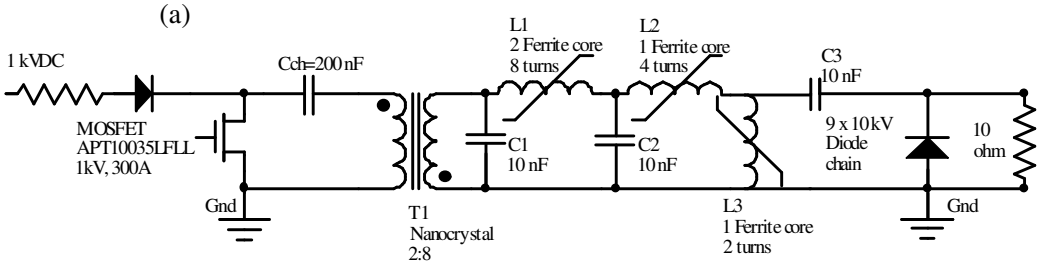

(b)

Figure 5.5 *(a) Circuit diagram of Magna-II pulse generator. (b) Photo of Magna-II pulse generator.*

In order to shorten the pulse width and increase amplitude, the system is modified in the following three aspects: (1) The LC resonant circuit is optimized to

generate shorter initial pulse; (2) The saturable transformer is replaced by two saturable inductors to gain independent control of forward and reverse pumping times; (3) more diode chains are put in parallel to relax the forward pumping requirement and further reduce the pre-pulse pedestal.

5.3.1 Modification of the Diode Opening Switch Stage

As discussed in chapter 5.2.2, switching speed of diodes degrades after series combination. Resistive loss during forward conducting phase also increases with the number of diode in series. To compensate for degradation caused by series connection, a diode block consisting of 9 parallel diode chains is used. By adopting this diode block, energy transfer efficiency during forward pumping increases and the pre-pulse pedestal during reverse pumping decreases significantly. The improvement by using more parallel chains is limited, so only 9 parallel chains are used. The maximum forward pumping time of this diode block is about 130 ns, which is slightly better than the 3 parallel chains design used in Magna-I but still not as good as a single diode (200 ns). Further research is needed to fully understand the effect of series/parallel combination on diode switching properties.

5.3.2 Modification of the Saturable Transformer Stage

In Magna-I, forward and reverse pumping of the diode stage is controlled by the saturable transformer T_2. In order to gain independent control, two saturable

inductors (L_2, L_3) are used. Here the forward pumping time is determined by the C_2, C_3 and saturated L_2 resonant circuit, while the reverse time is determined by C_3 and saturated L_3. By varying the number of turns in L_2 and L_3, the pumping of diode stage can be tuned.

In Magna-II system, another set of winding is added to L_2 and L_3 for core reset. Constant current is passed through the winding to generate reset magnetic field. This reset circuit not only makes the saturation of inductors more stable from pulse to pulse, but also increases the effective magnetic flux swing. This increase in ΔB_{sat} leads to less number of turns for the same saturation timing and less saturated inductance. With these modifications, the forward and reverse times reduced to 100 ns and 50 ns respectively.

5.3.3 Modification of the L-C Resonant Stage

A shorter initial pulse means less compression for a given output pulse width. The two limiting factors are switching speed of the IGBT and L-C resonant frequency. So the IGBT is replaced by fast MOSFET switch (APT10035 from Advanced Power Technology) in Magna-II design. LC resonant time is reduced by cut the run ratio in T_1 to 1:3 by using a 1kV voltage source instead of 300 V one. With a smaller turn ratio, both the leakage inductance and the effective capacitance on the primary are reduced. A nanocrystal (FT-3) core is used, which has a high

permeability at working frequency. This means high coupling coefficient of the transformer. Comparing with Magna-I, the width of initial pulse reduces from 1.5 μs to 700 ns.

5.3.4 Auxiliary circuit

Several auxiliary circuits like the capacitor bank, DC-DC converter and USB control interface are added, so that Magna-II can be a self sustain system.

Figure 5.6 is the block diagram of the new system and Figure 5.7 is the photo of the front panel.

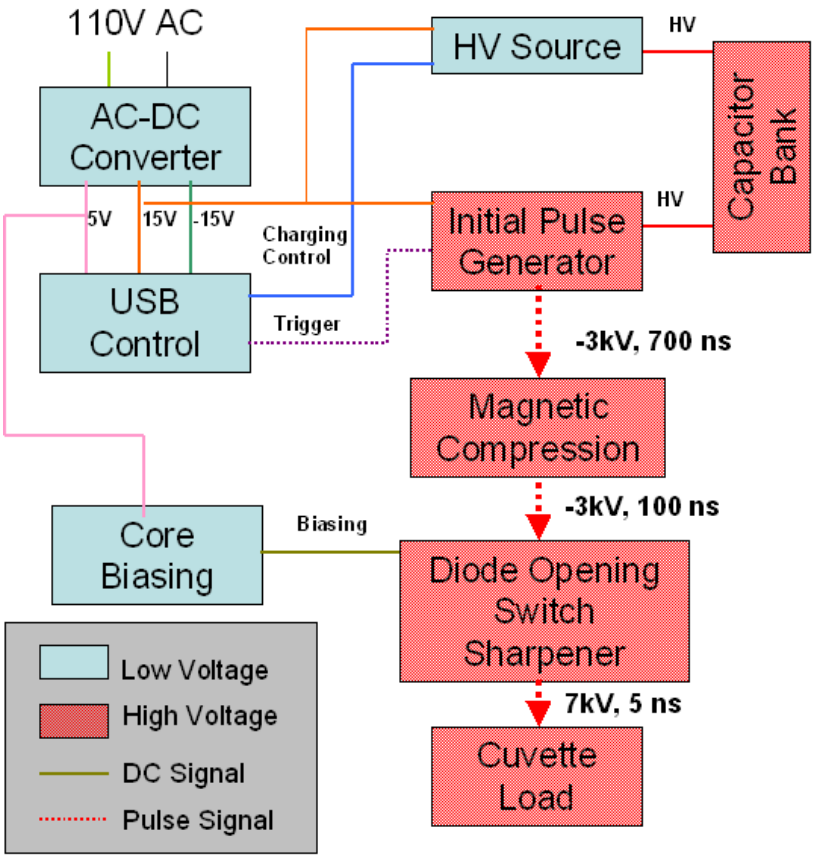

Figure 5.6 *Block diagram of Magna-II pulse generator*

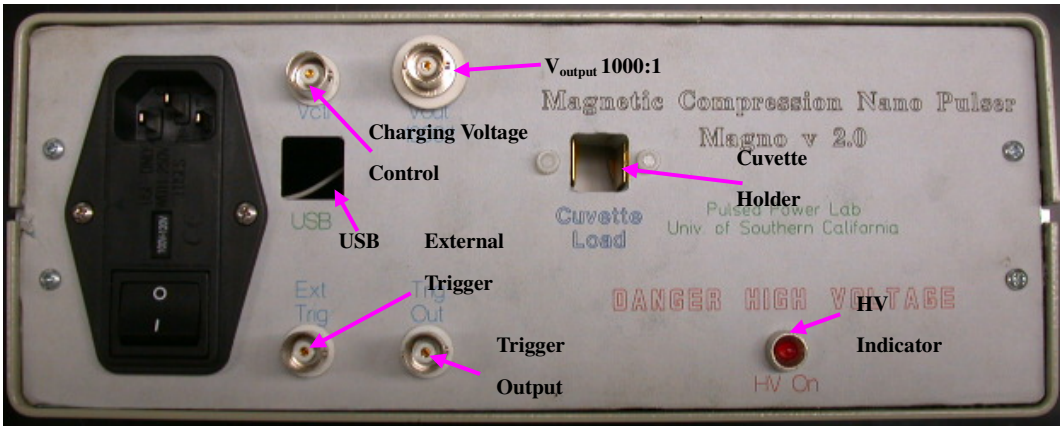

Figure 5.7 *Photo of Magna-II front panel*

5.3.5 Testing

Magna-II has a much shorter pulse width and higher amplitude comparing with Magna-I. For the same cuvette load, the pulse width is only about 5ns and amplitude is about 7.5 kV. Figure 5.8 is the output voltage waveform with a standard cuvette load.

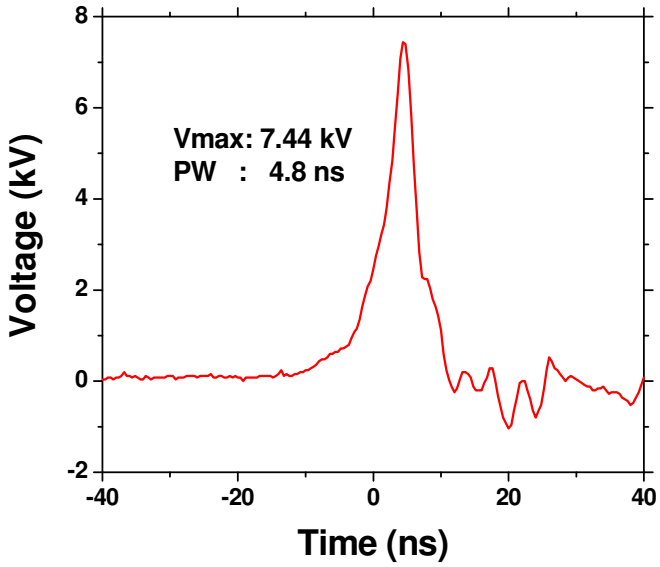

Figure 5.8 *Output voltage waveform of Magna-II with standard cuvette load*

5.4 Applications

The 7.5 kV 5ns pulses were applied on cell suspended in a cuvette. RPMI dye is used to characterize the permeability change of cells. The RPMI dye molecule can not get through cell membrane in normal situation. If the electric field changes the membrane property, dye molecule can diffuse into the cell. From the results we can see that on the control group, no dye molecule appears in the cell while the exposed cells light up under fluorescent microscope. This suggests the pulse generator successfully causes electroperturbation in cells.

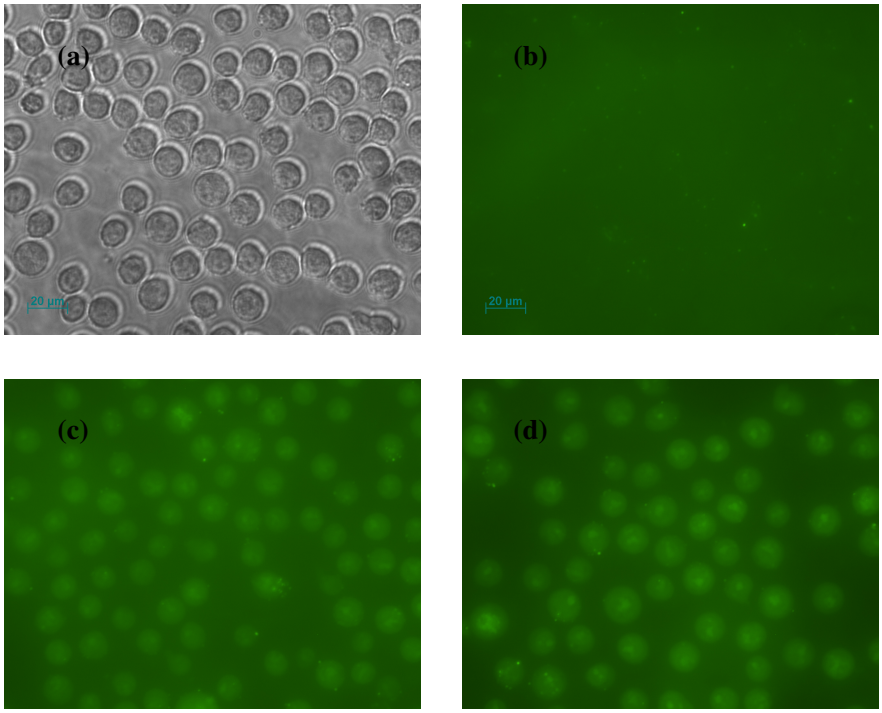

Figure 5.9 *Response of cells upon electrical pulses(a) white light image of control sample (0 pulse) (b)fluorescent image of control sample (c) fluorescent image of sample with 50 pulses (d) fluorescent image of sample with 100 pulses*

Chapter 6 DOS pulse generator for aerospace and automobile applications

Most of transient plasma ignition research done in out lab previously is based on the pseudospark pulse generator. The pseudospark pulser generates 75 ns, 90kV pulse into the 4" ignition chamber. Results of significant reduction in ignition delay and ignition pressure rise time were obtained with energy costs roughly comparable to traditional spark ignition methods (100 to 800mJ).

The main disadvantage of the existing pulse generator is that the pseudospark switch is fragile, large and expensive which may limit its application in some harsh environment like the aircraft and automobile ignition. Future ignition experiment in smaller chamber also requires a shorter pulse width. So a full solidstate pulse generator with 20 ns 60kV output is necessary.

6.1 Design goal

As mentioned in Chapter 1.3, due to the large electric field in the streamer head and large effective volume of the transient plasma (streamer in this case), the ignition using high voltage nanosecond electric pulse is studied in our laboratory. The current

experiment data strongly suggest the improvement of ignition in terms of ignition delay and ignition speed.

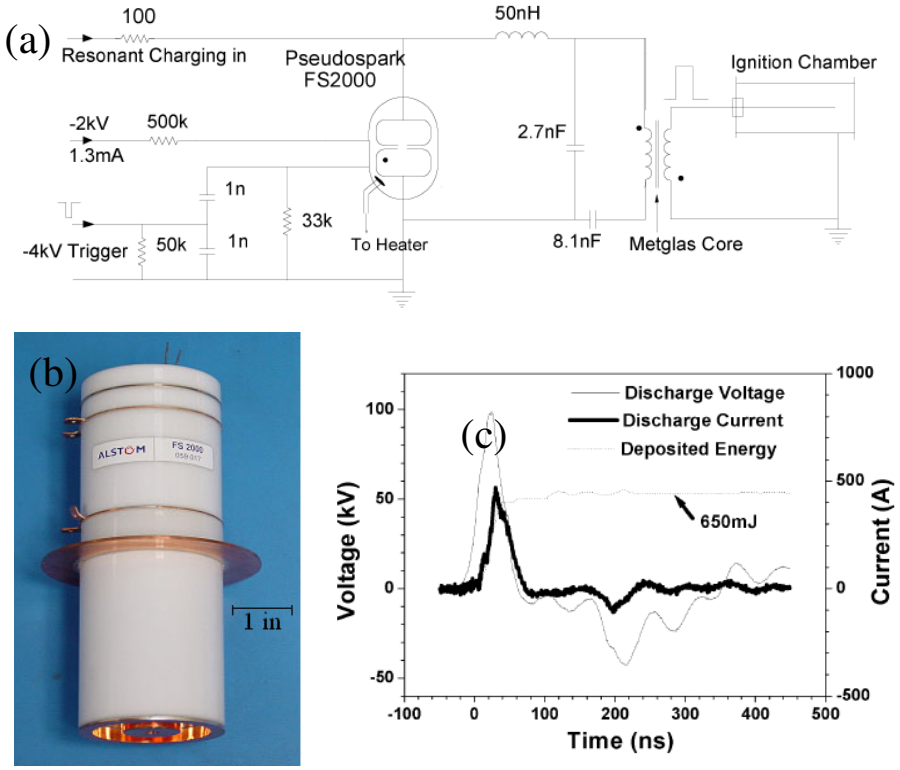

Figure 6.1 *(a) Circuit diagram of the pseudo-spark pulse generator (b) Photo of the pseudo-spark switch (c) output wave form of the pulse generator to the combustion chamber*

In the current experiment, the pulse generator based on pseudo-spark gas switch is utilized and good experimental results are got in both diesel engine and pulse detonation engine (PDE) ignition. And the circuit diagram of the pulse generator is shown on Figure 6.1 (a). The disadvantage of the pseudo-spark switch (Figure 6.1 (b)) is that the size of the switch is relatively large and the switch is fragile. The life time of the switch is also limited. An effort is spent on design a full solid-state pulse generator for this application.

6.2 Diode opening switch based design

The pulse generator consists of 3 units which are: resonant charging stage, magnetic compression stage, and DOS sharpener stage (Figure 6.2).

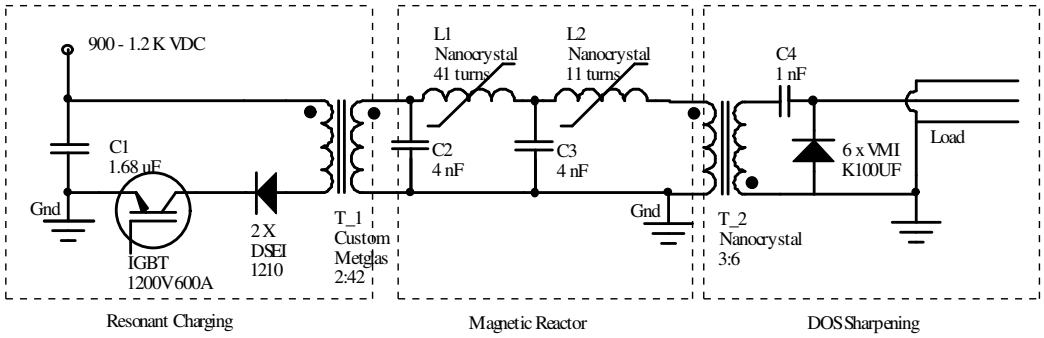

Figure 6.2 *Circuit diagram of DOS ignition pulse generator*

The resonant charging stage uses an L-C resonant circuit to drive a step up transformer. This way, the capacitor in the magnetic reactor can be charged to its working voltage (20 kV) using a low voltage solid-state switch. The magnetic compression stage then compresses the long pulse (2.3 μs) to about 200 ns to meet the forward pumping requirement of the DOS. A saturable transformer connecting the compression stage and DOS stage will establish a required reversed pumping current for DOS. Once the reverse current through the diode reaches its peak, the DOS will open and the current stored in the saturable core will be commuted to the load. So high voltage pulses are generated.

The system is fitted in a standard 19” rack mount enclosure with a height of 5.25” and depth of 17”. The overall weight is about 30 lbs.

6.2.1 Resonant Charging Stage

The resonant charging stage is formed by an IGBT switched L-C resonant circuit. Two DSEI-1210 diodes are used to block the reverse current through the IGBT. The charging voltage on storage capacitor C_1 ranges from 850 to 1.2k V. The output pulse amplitude will vary with this charging voltage. The step up transformer is built on a custom metglas core with OD=2” ID=1” H=1”. Once the IGBT turns on, the energy in C_1 will be transferred to C_2 and the voltage on C_2 will reach the working voltage (20 kV) for the magnetic reactor. The peak current through IGBT is 800 A, which is slightly larger than the rating. In short pulse operation, the IGBT survives and no damage occurs.

6.2.2 Magnetic Compression Stage

The magnetic compression stage has two magnetic reactors. Both of them work at 20 kV. The first one is formed by C_2, L_1 and C_3, which compresses 2.3 μs pulses into 420 ns with an efficiency of 74%. The second stage is formed by C_3, L_2, T_2, and C_4. It further compresses the pulse to 200 ns with efficiency of 58%. The efficiency of the second reactor is lower than the first one. The possible reasons are: 1. the loss in transformer T_2; 2. the loss of the core increases at high frequency.

Here, C_2 and C_3 are ceramic HV capacitor from TDK. And L_1 is built with 41 turns of awg 18 magnetic wires on a FT-3M core from MK-magnetics. The size of the core is OD=2", ID=1", H=1". While L_2 and T_2 are built on the same core, but instead of one H=1" core, two H=0.5" cores are stacked to reduce the loss through the cores. The winding on L_2 is formed by 11 turns of awg 18 HV silicone wire, while T_2 has 3 turn primary and 6 turn secondary winding with same HV wire.

The output of magnetic compression stage can be directly fed to a 200 Ω load. A typical output waveform is shown in Figure 6.3. The amplitude of pulse is 31 kV and the pulse width is about 100 ns when the input voltage is 1.2 kV.

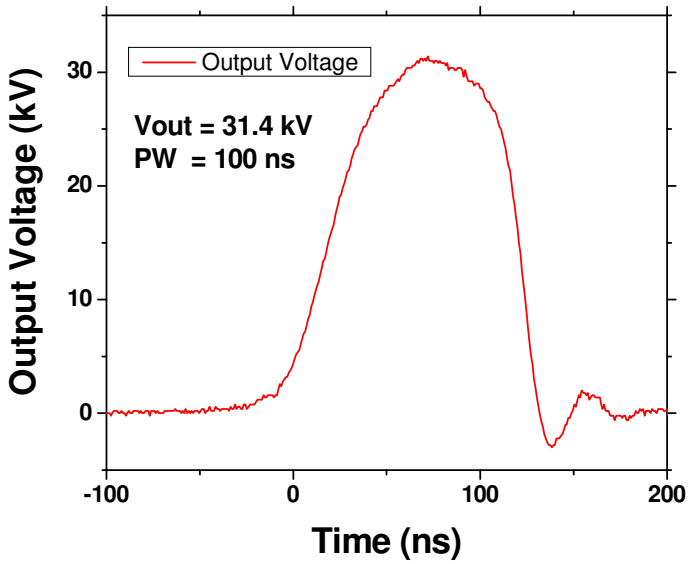

Figure 6.3 *Output from magnetic compression stage to 200 ohm load in the DOS ignition pulse generator*

6.2.3 Diode Opening Switch Sharpener Stage

The DOS is formed by 6 VMI K100UF diodes in series connection. The rated hold-off voltage of each diode is 10 kV and the current rating is 1.5 A DC.

The diode chain will be forward pumped with a 220 A 200 ns wide current pulse when C_4 is charged by previous stage. Then T_2 will saturate and the discharge process will force 510 A current flows reversely through DOS in 30ns. Once the reverse current reaches its peak value of 510A, the diode will interrupt the current and commute it to the load. About 300 A of current is switched to the load and generate 60 kV 20 ns pulse into the load. Although the diode is running under a pulsed current several hundred times higher than its DC rating, no damage occurs.

6.3 Operation

The system can work with DC high voltage source for low repetition rate (<5 Hz) operation and fly-back rapid charger for higher repetition rate (<1 kHz). Figure 6.4 shows a typical output waveform on 200 Ω resistive load . The amplitude of the pulse is 57.6 kV and pulse width (FWHM) is 18 ns.

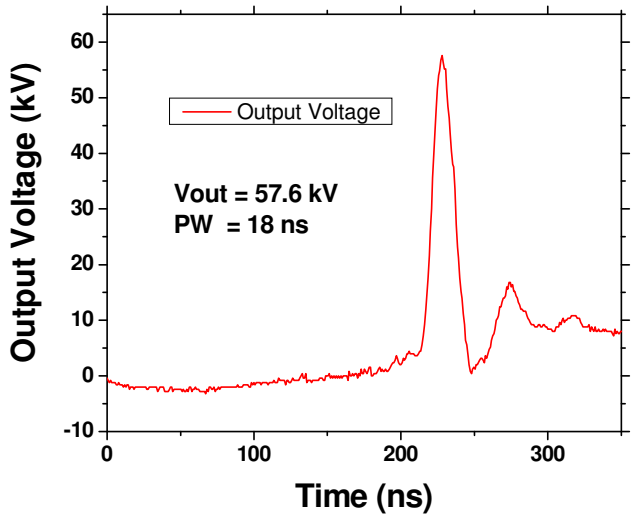

Figure 6.4 *Output pulse of DOS ignition pulse generator to 200 ohm load*

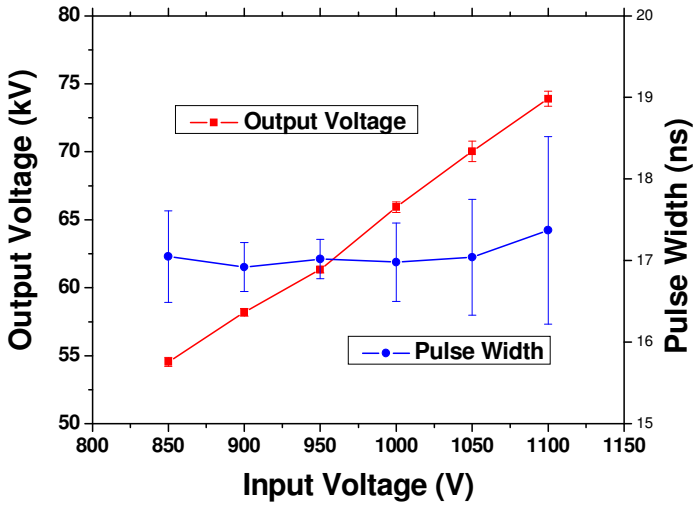

Figure 6.5 *Output pulse amplitude and width vs different charging voltage of DOS ignition pulse generator*

The output pulse amplitude can be tuned by charging voltage on C_1. Figure 6.5 shows the output amplitude and pulse width under different charging voltages. From this control curve, we can see that the output voltage can change from 55 kV to 75

kV with small variations in pulse width. The maximum variation in the pulse width is about 1.5 ns (@1.2 kV charging) and the average pulse width is about 17 ns.

The overall efficiency is only about 25%. The loss is mainly introduced by the transformers.

6.4 Application

This pulse generator is used in a single cylinder internal combustion engine.

Figure 6.6 shows the discharge system in this application. The anode is a 2.2 mm diameter 12 mm long rod with 45 thread/mm thread. Length of the anode is 12 mm. Cathode is a brass cylinder with inner diameter of 15 mm.

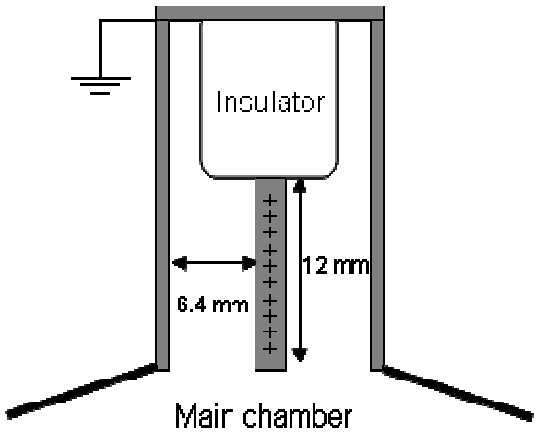

Figure 6.6 *Electrode schematic of the ignition plug*

The 20 ns pulse allowed a substantial increase in the applied electric field while holding off spark breakdown. The mean electron energy scales with reduced electric field. The higher applied voltage of the 20 ns pulse increased the reduced electric field and thus the number of high energy electrons capable of dissociation and

ionization, which then increased number of free radicals that initially seed the discharge volume. As shown in Figure 6.7, peak pressure achieved with the 20 ns pulse, was 20% greater than that from spark gap, indicating a larger net heat release. This result correlates well with previous work done, and is indicative of reduced heat loss to the walls.

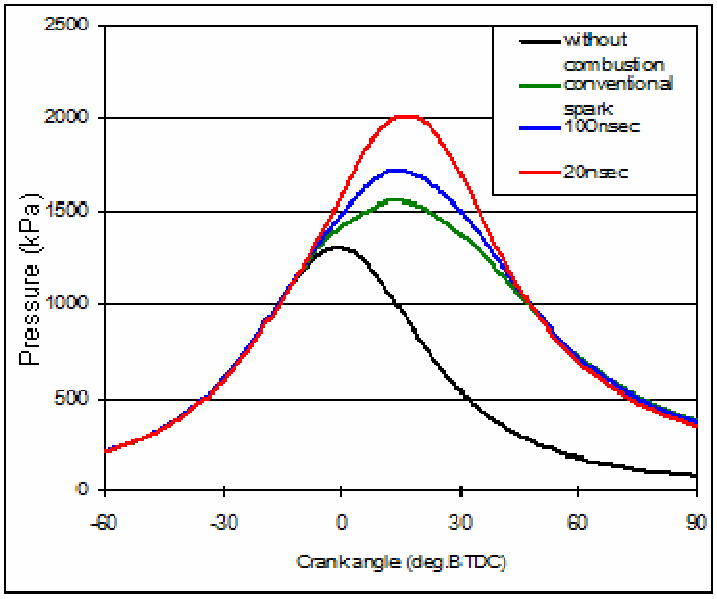

Figure 6.7 *Pressure v. crank angle at Φ=.72.*

Chapter 7 Dual-pulse design for TPI

One problem of the solid state pulser presented in chapter 6 is the cost of magnetic materials. The size and price of the core for magnetic compression largely depends on the energy transferred. In order to transfer about 1 J energy (500mJ delivered to the chamber with 50% efficiency), a core of about 1 kg is required for every compression stage. Then the system will be bulky and expensive.

Inspired by the observation from transient plasma imaging experiment and the design of ozone generator circuit, a new concept for the aeronautic and automobile ignition application is proposed. The real-time images suggest the streamer will not start initiated until the anode voltage reaches a certain threshold. So a slow rising pulse (no compression needed) can be used to charge the chamber to 40 kV, which is lower than the threshold voltage for streamer generation. Then a sharp pulse of 20 ns 40 kV is applied on top of the slow pulse. The voltage of combined pulse will exceed the threshold and streamers will be generated. Besides the advantage of using a lower voltage switch, the pulse adding topology is more efficient since part of the energy is transferred through the low loss long pulse.

7.1 Real-time streamer imaging

To get better understanding of how a streamer is formed when a voltage pulse applied, a high speed camera is used to take real-time image with voltage and current measurement. The chamber is a 4" diameter stainless steel cylinder, which is also works as a discharge cathode. The anode is a 1.3" brass gear which is connected to the output of pseudo-spark pulse generator. Figure 7.1 shows the voltage and current on the discharge structure. A series of images are taken at different time relative to the peak of voltage. The inset of Figure 7.1 is the image taken 16 ns before the peak when the voltage across chamber reaches 50 kV. On this image, streamers are just initiated on the teeth of gear electrode, while no streamer can be found on any image taken before this. This observation suggests the existence of a threshold voltage (50 kV in this case) for streamer formation.

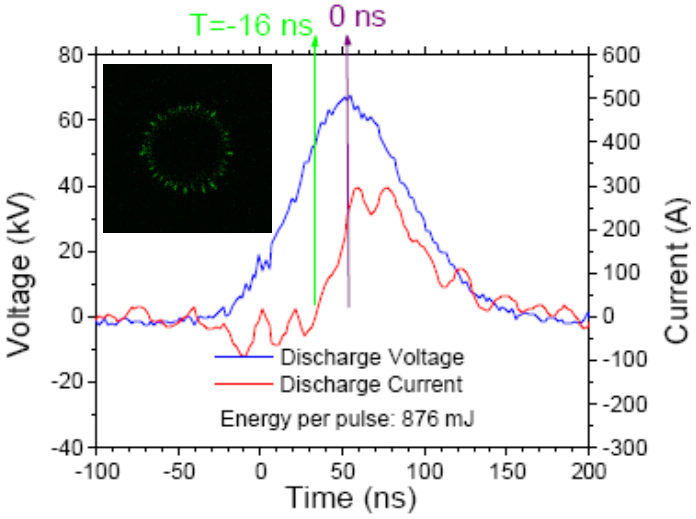

Figure 7.1 *I-V measurement and image of discharge chamber*

This observation suggests voltage rise prior to threshold may not be critical for streamer formation. The anode can stay at a voltage lower than threshold first. Then streamers can be formed by a lower amplitude pulse atop it. But if the anode stays at high voltage for a long time, not only safety will be a big concern but also the leakage will be severe. If the anode can be charged to sub-threshold voltage right before the arriving of fast rise pulse, these two concerns will be easily solved.

7.2 Principle of pulse adding

A pulse adding topology is shown in Figure 7.2. In this scheme, a slow rise pulse is used to bring the anode to near threshold voltage. Then a fast pulse is added through a coupling capacitor. The combined pulse has a fast rise time above threshold, which will be able to generator streamer efficiently.

The coupling capacitor also works as a storage capacitor for slow rise pulse. The slow pulse charges the capacitor to sub-threshold voltage and energy is then stored. When the fast pulse initiates discharge process, part or all of the stored energy will deliver to the load. For same total discharge energy, less energy is needed to be carried by fast pulse. A fast pulse system generally consists of more compression stages, which implies a large loss. So the energy transfer efficiency will be improved since part of energy transferred through low loss slow pulse.

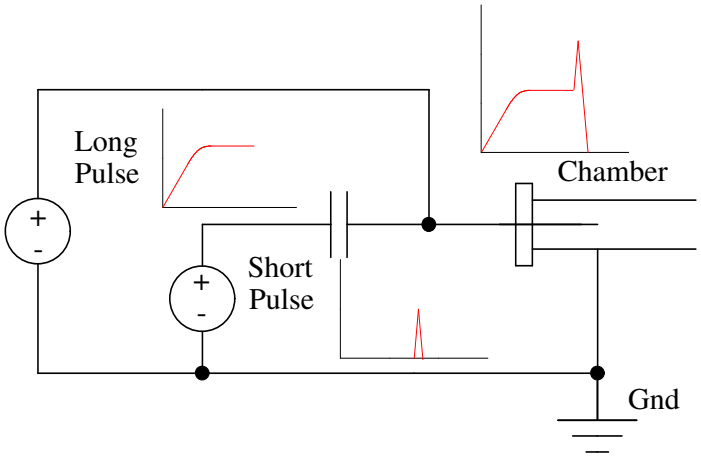

Figure 7.2 *A schematic of pulse adding topology*

Another advantage of this scheme is the requirement for switch in fast pulse system is relaxed. The amplitude of the short pulse is reduced by the amount of slow pulse amplitude. In other word, the same fast switch can be used to generate a higher peak voltage on the anode.

7.3 Design of dual pulse system

As illustrated in Figure 7.2, the pulse adding system consists of three main subunits: the slow rise pulse generator, the fast rise pulse generator and the adding unit. The circuit diagram is shown on Figure 7.3.

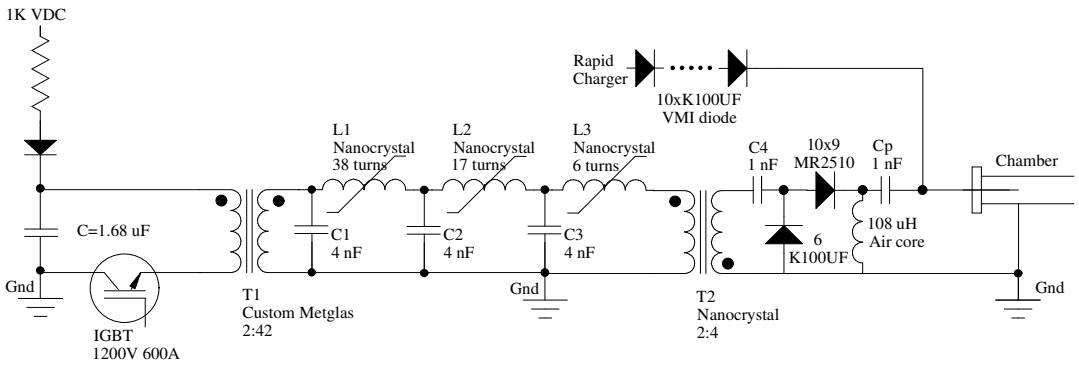

Figure 7.3 *Circuit diagram of pulse adding system*

7.3.1 Slow rise pulse generator

A flyback resonant charger is used to generate slow rise long pulse. The charger has 3 major components: capacitor bank, switch and flyback transformer.

A 6.6 mF capacitor is used as capacitor bank, which is charged by rectified 3-phase 208 V. The capacitor is connected to a FUJI IGBT (1MB1600PX-140) through primary of a flyback transformer. The HV flyback transformer is wound on a 4” ID, 6” OD 2” high toroid core with 1.2 cm gap. The core is made of 4 mil silicon iron tape and has a turn ratio of 8:375. The IGBT is closed to charge transformer primary. Then the IGBT will be opened so that the energy stored in transformer primary will be delivered to the load on the secondary.

The charger is tested in the circuit and Figure 7.4 (a) is the voltage at the right node of Cp. The 1nF coupling capacitor is charged to 32 kV in about 30 μs.

7.3.2 Fast rise pulse generator

A magnetic reactor driven diode opening switch pulse generator is used to deliver fast rise pulse. This pulser is similar to the pulse generator presented in chapter 6. Here is a brief description of its working principle: The closing of high voltage IGBT initiates a 2 μs voltage rising in the secondary of step-up transformer T_1, which will charge C_1 to 20 kV. The inductor L_1, L_2 and L_3 are wound on 2" OD, 1" ID, 1" High, finemat nanocrystal core from MK-Magnetics. The number of turns in L_1, L_2, L_3 is carefully tuned so that they will saturate respectively once C_1, C_2, C_3 charged to its peak value. C_1, L_1, C_2, L_2, C_3, L_3 forms a three-stage magnetic compression stage, which will compress the 2 μs pulse initiated by IGBT to about 100 ns. Then the pulse will feed to C_4 through forward biased diode. The transformer T_2 is designed to saturate once all the energy transferred from C_3 to C_4, and the current will flow reversely through diode chain formed by 6 VMI (K100UF) diode. The reverse recovery of the diode will work as an opening switch, which commutes the current in saturated T_2 to the load.

The output of this unit is tested using a 200 ohm high voltage resistor load. The resistance is approximately that of the discharge load during streamer phase. The waveform is shown on Figure 7.3. (b)

7.3.3 Pulse adding unit

The adding unit consists of a high voltage capacitor acting as coupling capacitor for fast pulse and storage capacitor for slow pulse. To hold high voltage of the combined pulse, two 40 kV 2 nF ceramic TDK high voltage capacitor is connected in serial as Cp.

Ten 10 kV VMI diodes are connected in serial between the rapid charger and the anode of the discharge chamber, which will isolate the fast pulse form the rapid charger. A 10×9 diode array is inserted between the left end of Cp to the output of the fast pulse generator which will prevent current flow to fast pulse generator during slow pulse. Saturation of T_2 and the initial charge in diode opening switch will be largely affected by any charge flows during slow pulse.

An air core inductor is used to provide a grounding path for the slow pulse. The inductance value is selected so that it will short the left end of Cp to ground when the slow pulse charges Cp and isolate the left end from ground when fast pulse arrives. The large difference in pulse rise time gives a broad range of selection. In this system, a 108 μH air core inductor is used.

7.4 Operation

Experimental results are shown in Figure 7.4. The system is first operated with one pulse a time. Figure 7.4 (a) is the waveform with only the slow rising pulse. The

rapid charger successfully increases the voltage on the load to 32 kV in about 30 μs. And the voltage can stay at 32 kV without any arcing or voltage drop. The fast pulse is applied on the chamber with a 200 ohm load, and the waveform is shown on Figure 4 (b). Then this two pulse generator is synchronized and two pulses are added together as shown in Figure 4 (c). Figure 4 (d) is a detail view of voltage waveform after fast pulse.

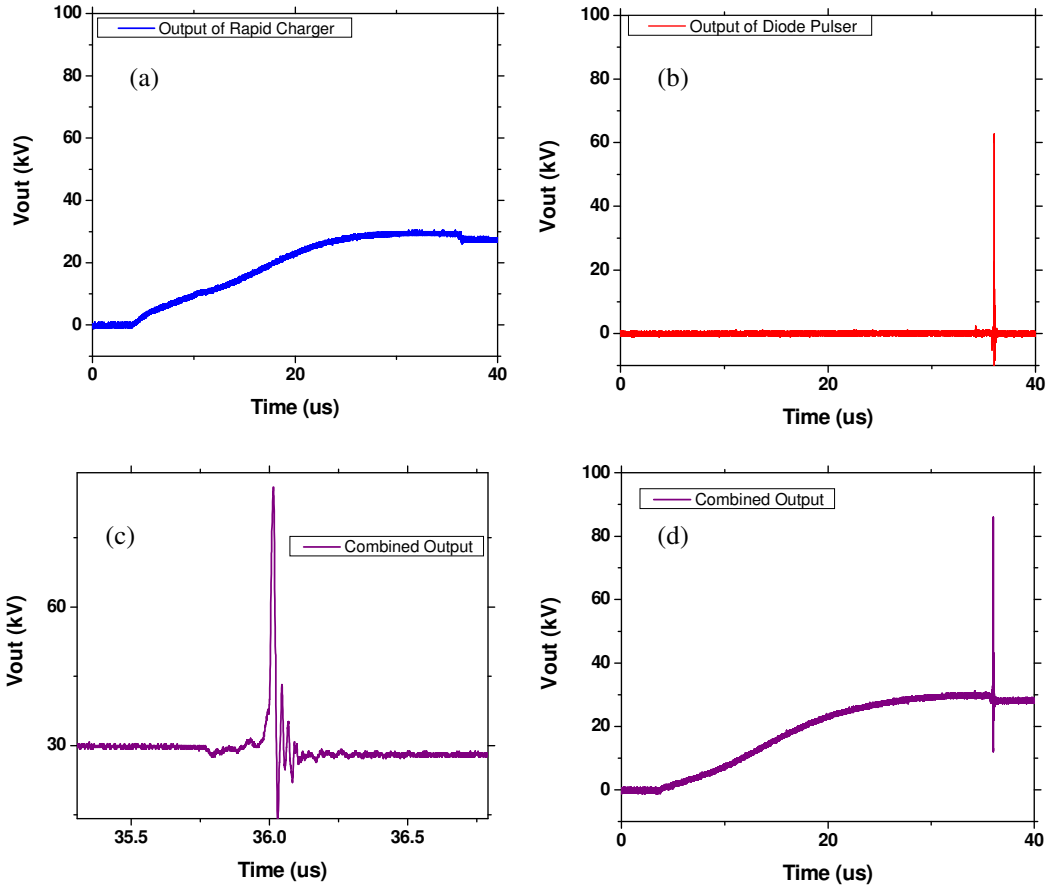

Figure 7.4 *Output waveform of pulse adding system (a) output voltage with only slow rise pulse; (b) output voltage with only fast pulse; (c) added pulse; (d) zoom in of added pulse, pulse amplitude 86 kV, width about 20 ns.*

The combined pulse is then applied on a discharge chamber. The anode is a 3" diameter stainless steel cylinder, and the center is cathode formed by 1/8 diameter threaded rod. The image is taken by long time exposure and the streamer in the whole volume can be clearly seen.

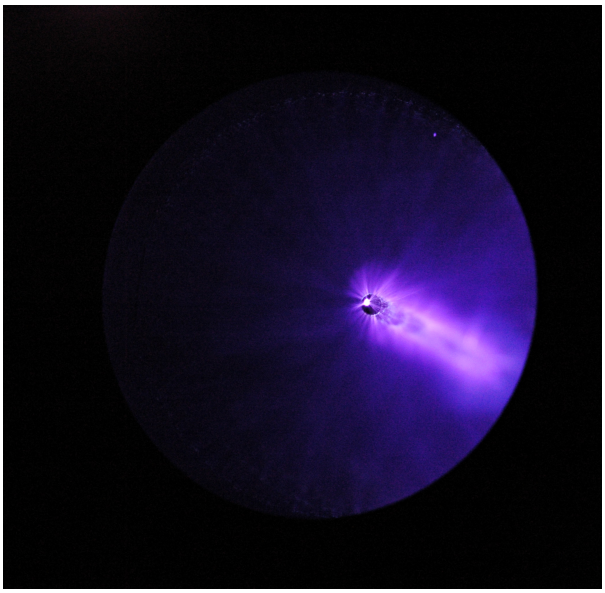

Figure 7.5 *Streamer image with pulse adding system*

Streamer image also shows the short pulse alone will not able to generate any visible streamer. So the pulse adding technique reduced the requirement for output voltage.

The pulse adding system is also tested with a stoichiometric methane-air mixture ignition. CH_4 is used as fuel and compressed air as the oxidizer. The initial pressure of the air/fuel mixture is 1 atm. Here a steel pin is attached to the center electrode and the distance between the pin to the outer cylinder is adjustable. The

discharge geometry is like point-plane. A pseudospark pulse generator is used here as a baseline to comparing ignition data. The pressure curve of the chamber characterized the ignition process. Two important factors are the rising time of the pressure cure and the peak pressure. The rising time characterized the speed of combustion and the peak pressure is related to how the combustion energy can be efficiently used. The rule is: short rise time and high peak pressure suggest a better (clean, fast) combustion.

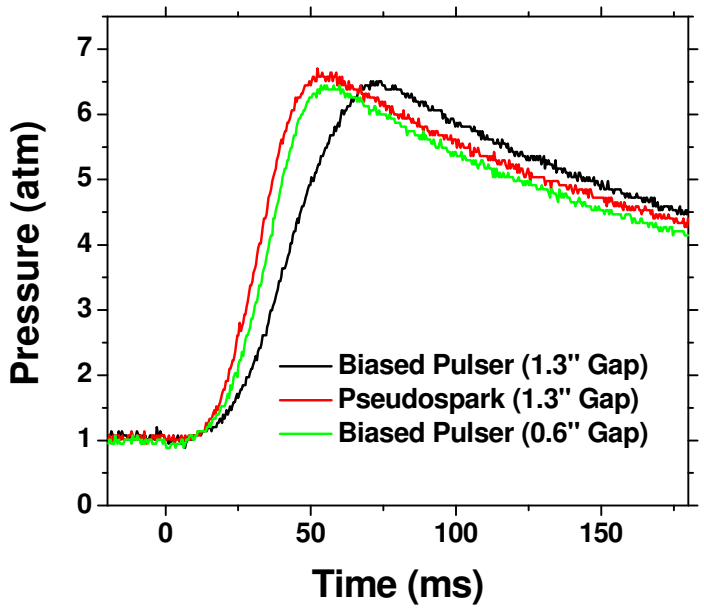

Figure 7.6 *Pressure change to time during combustion using pulse adding system*

The pressure waveforms in Figure 7.6 indicate at same gap distance of 1.3”, 50 ns 60 kV pulse generated by pseudospark pulser has a better ignition performance

than the 20 ns 65 kV combined pulse. By reducing the gap to 0.6”, the performance will be comparable.

Chapter 8 Outlook

For cost and reliability consideration, newly developed pulsed power system is mostly based on solid state components. In modern designs, gas switches, which were widely used in old generation of pulsed power circuits, are only used in such cases where solid state alternative is not available. The trend of moving into solid state era is quite clear.

Here some thoughts of future development in solid state pulsed power systems will be presented.

8.1 New device optimized for pulsed power applications

The key element for solid state pulsed power system is the switch. Comparing with traditional gas switches, the power handling capability of the solid state switches is lower and the switching speed is also slower.

Current “power” solid state devices are designed for high average power, where heat dissipation is the major concern. But the average power in a pulsed power system is much low than its peak power, which means heat dissipation in the switch is not the limiting factor. So the bulky heat sinks in most power switches are not

helpful for pulsed power applications. On the contrary, the large spacing required by efficient heat transfer introduces large parasitic capacitance and inductance, which will slow down the device.

By removing the large heat sink and using a compact package, the size of switches can be shrunk dramatically. Figure 8.1 shows an example of such device. For similar voltage rating, traditional power device can be as large as 5.2”x5.5”x1”. This package successfully reduces the size of switches.

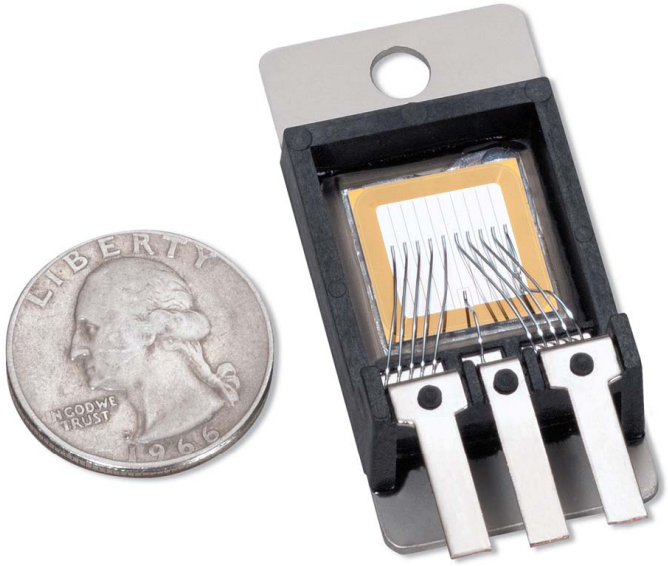

Figure 8.1 *PowerEx pulsed power high voltage IGBT*

In pulsed power applications, the switches will experience high di/dt. So, the voltage drop on parasitic inductance can be significant, which may be the limiting element in high speed switching. A package with small inductance is preferred for pulsed power, which is next thing to optimize. A large potion of package inductance

comes from bonding wire. The size of bonding wire is normally very small, which can be the bottle neck of the current flow. One simple solution is to use multiple bonding wires. To further reduce package inductance, the package used in radio frequency IC will be a good choice. BGA type package may be very helpful in this case.

Without any change in die fabrication, simple change in package will greatly improve the performance of device in pulsed power condition.

Of course, adoption of high band gap high mobility material for device fabrication will give a significant improvement in hold off voltage and switching speed. Among those materials, SiC may be the most promising one for pulsed power applications.

8.2 Characterize devices under pulsed power condition

The circuit element is normally characterized in low voltage low frequency conditions. The device can perform differently in pulsed power system.

A switch element may have several times higher current handling capability in pulsed mode than continuous mode. A good example is the VMI diode used in ignition pulse generator (discussed in chapter 6.2.3). The diode is rated 1.5 A in continuous operation. In the generator, it conducts 220 A 100 ns pulse without any

problem. An accurate “pulsed power” datasheet of switch will be very helpful in device selection for cost reduction purpose.

Another important element to be characterized is the load. Efficient energy delivery can only be achieved if the load is well understood. For example, in ignition applications, the goal is to deliver energy into the gas mixture. Once arc is formed, energy can not be efficiently delivered due to its low impedance. So, introduction of transient plasma ignition shows observable improvement by avoiding such losses. Further understanding of streamer formation and streamer-arc transaction process leads to the pulse adding system presented in chapter 7. Some preliminary experiments suggest a power law relation of the gas pressure, average impedance and applied voltage. Better understanding of streamer formation dynamics based on further experiments will provide a guide to optimize pulse shape for different ignition condition.

8.3 Generate simulation model of pulsed power components

The design of pulsed power system is mostly based on trail and error. The most important reason is lack of accurate device model under pulsed power condition. Most of the circuit model only deals with low voltage low power applications, which will not take the nonlinear behavior of the circuit element into consideration. Most of

the pulse power system is built using expensive components or custom parts for which trail and error may be unacceptable.

It is very hard to get accurate measurement for a high voltage wide band system. So a method to extract model parameters based on low voltage measurement will be important. This method will also be very useful for device screening and matching.

With an appropriate circuit model, optimization of the system will be much easier. And finding the critical element in a complex pulsed power system will be largely simplified.

There are analytic models of some components like Diode Opening Switches, gas discharge chamber. These models are normally based on fundamental physics process involved and are time consuming when simulated. A good starting point is to rewrite these models in circuit simulation software like SPICE. Such work for discharge system was done by a research group in Israel.

References

Richard. H. Adler, "Pulse power formulary", North Star Research Corporation.

E. A. Alichkin, S. K. Lyubutin, A. V. Ponomarev, S. N. Rukin, and B. G. Slovikovskii, "Formation of short pulses witha subnanosecond rist tiem and a peak power of up to 1 GW by a semicondutor avalanche sharpener", Instruments and Experimental Techniques, Vol. 45(4), pp. 535-539, 2002.

D. M. Barrett, "Core Reset Considerations in Magnetic Pulser Compression Networks", Proc. 10th IEEE International Pulsed Power Conference, pp1160-1165, Albuqureque, New Mexico, 1995.

E. M. Bazeluan, Y. P. Raizer, "Spark discharge", CRC PRess, Boca Raton, New York, 1997.

S.J. Beebe, P.M. Fox, L.J. Rec, K. Somers, R.H. Stark and K.H. Schoenbach "Nanosecond Pulsed Electric Field (nspef) Effects on Cells and Tissues: Apoptosis Induction and Tumor Growth Inhibition," Invited Paper, IEEE Trans. Plasma Science 30, 286 (2002).

S. J. Beebe, P. M. Fox, L. J. Rec, L. K. Willis, and K. H. Schoenbach, FASEB J. vol. 17, pp1493–1495, June 2003.

M. Behrend, A. Kuthi, X. Gu, P. T. Vernier, L. Marcu, C. M. Craft, M. A. Gundersen, "Pulse generators for pulsed electric field exposure of biological cells and tissues", IEEE Tran. Dielectrics & Electrical Insulation, vol. 10, pp820-825, Oct. 2003.

Hansjochen Benda, and Eberhard Spenke, "Reverse recovery processes in silican power rectifiers", Proc. IEEE, vol. 55(8), pp1331-1354, Aug 1967

H. Bluhm, "Pulsed power systems, Principles and applications", Springer 2006.

Michael John Chudobiak, "New approaches for designing high voltage, high current silicon step recovery diodes for pulse sharpening applications", Ph. D. Desertation. Carleton University, Ottawa, Ontario, Canada, 1996.

Michael J. Chudobiak, David J. Walkey, "Forward Transient Charge Injection in psn Diodes at Medium to High Injection Levels", IEEE Trans. on Electron Devices, Vol.44(1), pp190-194, Jan 1997.

E. G. Cook, "Review of solid-state modulators", XX International Linac Conference, Montery, California pp.663-667.

E. G. Cook, “Magnetic Compression Circuits and Kicker Dirver Options”, Cooling Ring Kicker Meeting, Mar. 2002, http://www.fnal.gov/projects/muon_collider/eexchange/Meetings/Kickers/Cook.pdf

S. A. Darznek, G. A. Mesyats, and S. N. Rukin, "Dynamics of electron-hole plasma in semiconductor opening switches for ultradense currents", Tech. Phys. vol.42(10), pp.1170-1175, Oct. 1997.

S. A. Darznek, S. N. Rukin, and S. N. Tsiranov, "Effect of sturcture doping profile on the current switching-off process in power semicondutor opening switches", Tehcnical Physics, vol. 45(4), pp. 436-442, 2000.

R. J. Focia, E. Schamiloglu, and C. B. Fleddermann, "Simple techniques for the generation of high peak power pulses with nanosecond and subnanosecond rist times", Rev. Sci. Instrum. vol. 67(7), pp. 2626-2629, Jul. 1996.

I. V. Grekhov, V. M. Efanov, A. F. Kardo-sysoev, and S. V. Shenderey, "Power drift setp recovery diodes (DSRD)", Solid-State Electronics, Vol. 28(6), pp. 597-599, 1985.

I. V. Grekhov and G. A. Mesyats, "Physical Basis for High-Power Semiconductor Nanosecond Opening Switches, IEEE Tran. on Plasma Scien., Vol 28, pp1540-1544, October, 2000.

I. V. Grekhov, A. K. Kozlov, S. V. Korotkov, A. L. Stepanyants, and D. V. Khristyuk, "Formation of high-power pulses of nanosecond duration by generators on revers switch-on dynistors with sharpening circuits based on diode opening switches", Instruments and Experimental Techniques, Vol. 45(4), pp. 530-534, 2002.

I. V. Grekhov, G. A. Mesyats, "Nanosecond semicondutor diodes for pulsed power switching", Physics-Uspekhi, vol. 48(7), pp. 703-712, 2005.

W. Hartmann, Th. Hammer, T. Kishimoto, M. Roemheld, A. Safitri, “Ozone Generation in a Wire-Plate Pulsed Corona Plasma Reactor”, 15th IEEE Pulsed Power Conference, Monterey, CA, Jun 13-17, 2005.

R. P. Joshi, Q. Hu, K. H. Schoenbach, and S. J. Beebe, “Simulations of Electroporation Dynamics and Shape Deformations in Biological Cells Subjected to High Voltage Pulses,” IEEE Trans. Plasma Science 30, 1536 (2002).

S. V. Korotkov, "Switching possibilities of reverse switched-on dynistors and principles of RSD circuitry (Review)", Instruments and Experimental Techniqures, Vol. 45(4), pp. 437-470, 2002.

S. D. Korovin, S. K. Lyubutin, G. A. Mesyats, V. V. Rostov, S. N. Rukin, B. G. Slovikovsky, M. R. Ul'maskulov, K. A. Sharypov, V. G. Shpak, S. A. Shunailov, and M. I. Yalandin, "Generation of subnanosecond 10-GHz pulses in high peak and high average power mode", Technical Physics Letter, vol. 30(9), pp. 719-723, 2004.

V. A. Kozlov, A. F. Kardo-Sysoev, and V. I. Brylevskii, "Impact Ionization Wave Breakdown of Drift Step Recovery DIodes", Semiconductors, Vol. 35(5), pp. 608-611, 2001.

A. Kuthi, P. Gabrielson, M. Behrend and M. Gundersen, “Nanosecond Pulse Generator Using a Fast Recovery Diode,” 26th IEEE Power Modulator Conference, San Francisco, CA, May 23-26, 2004.

A. S. Kyuregyan, "Theory of drift step-recovery diodes", Technical Physics, Vol. 49(6), pp. 720-727, 2004.

S. K. Lyubutin, G. A. Mesyats, S. N. Rukin and B. G. Slovikovskii, "Repetitive Nanosecond All-Solid-State Pulsers Based on SOS Diodes", Proc. 11th IEEE International Pulsed Power Conference, pp992-998, Baltimore, Maryland, 1997.

John Mankowski, Magne Kristiansen, "A review of short pulse generator technology", IEEE Trans. on Plasma Science, Vol. 28(1), pp. 102-108, Feb. 2000.

J. C. Martin, “Nanosecond pulse techniques,” Proc. IEEE, vol. 80, pp. 934–945, June 1992.

Gennady. A. Mesyats, “Pulsed power”, Kluwer Academic/ Plenum Publishers, New York, 2005.

N. Mohan, T. M. Undeland, and W. P. Robbins, Power Electronics (Wiley, 1995).

E. Neumann, A. E. Sowers and C. A. Jardan, “Electroporation and electrofusion in cell biology”, Plenum Press, New York, NY 1989.

D. O’Brien, “EC capacitors Diliver Hihg Capacitance in a Small Size”, Mar. 2001. http://powerelectronics.com/mag/power_ec_capacitors_deliver/

Katarzyna Opalska, and Jerzy Baranowski, "A charge model of step recovery diode for CAD", IEEE MTT-S Digest, pp1503-1506,1997.

S. T. Pai and Qi Zhang, “Introduction to high power pulse technology”, World Scientific 1995.

A. J. M. Pemen, I. V. Grekhov, E. J. M. van Heesch, K. Yan, S. A. Nair, S. V. Korotkov, "Pulsed corona generation using a diode-based pulsed power generator", Review of Scientific Instruments, vol. 74(10), pp.4361-4365, Oct. 2003.

V. Puchkarev and M. Gundersen, "Energy efficient plasma procession of gaseous emission using short pulses", Appl. Phys. Lett. 71(23), 3364 (1997).

V. Puchkarev and M. Gundersen, "Power modulators for control of transient plasmas for environmental applications", 23rd International Power Modulator Symposium, Rancho Mirage, CA June 22-25, 1998.

Y. P. Raizer, "Gas Discharge Physics", Springer-Verlag, Berlin, 1997.

Stephan Roche, "Solid state pulsed power systems"

S. N. Rukni, and S. N. Tsyranov, "The effect of a space charge on the opertation of a high-power semiconductor current interrupter", Technical Physics Letters, Vol. 30(1), pp. 19-22, 2004.

E Schamiloglu, R. J. Barker, and M. Gundersen, “Modern Pulsed Power: Charlie Martin and Beyond”, Proc. IEEE, vol. 92, pp1014-1020, July 2004.

P. W. Smith, "Transient Electronics: Pulsed Circuit Technology", J. Wiley, 2002.

T. Tang, F. Wang, A. Kuthi and M. Gundersen, “Nanosecond Pulse Generator Using Diode Opening Switch for Cell Electroperturbation Studies ”, 15th IEEE Pulsed Power Conference, Monterey, CA, Jun 13-17, 2005

Y. Teromoto, D. Deguchi, I. V. Lisitsyn, T. Namihira, S. Katsuki and H. Akiyama, "All-solid-state triggerless repetitive pulsed power generator utilizing a semiconductor opening switch", Review of Scientific Instruments, Vol. 72, pp. 4464-4468, December, 2001.

P. T. Vernier, Y. Sun, L. Marcu, S. Salemi, C. M. Craft, and M. A. Gundersen, “Field-Dependent, Non-Invasive Intracellular Electroperturbation of Human Lymphocytes,” Workshop on High-Field Effects and Fast Pulse Responses in Bio-Systems, IEEE Conference on Electrical Insulation and Dielectric Phenomena, October 19–22, 2003, Albuquerque, NM.

P. T. Vernier, A. Li, L. Marcu, C. M. Craft, and M. A. Gundersen, “Ultrashort Pulsed Electric Fields Induce Membrane Phospholipid Translocation and Caspase Activation: Differential Sensitivities of Jurkat T Lymphoblasts and Rat Glioma C6 Cells”, IEEE Trans. on Dielectrics and Insulation, 10: 795-809, 2003.

F. Wang, C. Jiang, A. Kuthi and M. Gundersen, J. Sinibaldi and C. Brophy, "Transient Plasma Igntion of Hydrocarbon-Air Mixtures in Pulse Detonation Engines", 42nd AIAA Aerospace Sciences Metting and Exhibit, Reno, NV, Jan 5-8, 2004. AIAA paper 2004-834

F. Wang, A. Kuthi and M. A. Gundersen, "Compact High Repetition Rate Pseudospark Pulse Generator", IEEE Tran. on Plasma Science, Vol. 33, pp1177-1181, August 2005.

F. Wang, A. Kuthi, C. Jiang and M. Gundersen, "Technology for Transient Plasma Ignition," 43rd AIAA Aerospace Sciences Meeting and Exhibit, Reno, NV, Jan 10-13, 2005. AIAA Paper 2005-0951.

“What is a capacitor?”, http://www.rohm.com/en/cap/cap_what3.html

Datasheet of Series T-508 Spark Gap Switches, L-3 Communications,
http://www.titanpsd.com/PDFs/T-508.pdf

Datasheet of 7665 Hydrogen Thyratron, E2V Inc,
http://www.e2v.com/download.cfm?type=document&document=37

MR2510 datasheet, On Semiconductor,
http://www.onsemi.com/pub/Collateral/MR2500-D.PDF